Stony Brook University

Physical Characteristics of Bering Sea Zooplankton and Their Use to Parameterize an Acoustic Scattering Model for Euphausiids

A Thesis Presented

by

Joy Nicole Smith

to

The Graduate School

in Partial Fulfillment of the

Requirements

for the Degree of

Master of Science

in

Marine and Atmospheric Science

Stony Brook University

August 2010

Stony Brook University

The Graduate School

Joy Nicole Smith

We, the thesis committee for the above candidate for the Master of Science degree, hereby recommend acceptance of this thesis.

Dr. Joseph D. Warren – Thesis Advisor
Assistant Professor
Marine and Atmospheric Science

Dr. Stephan B. Munch
Assistant Professor
Marine and Atmospheric Science

Dr. Patrick H. Ressler
Research Fishery Biologist
National Marine Fisheries Service,
Alaska Fisheries Science Center

This thesis is accepted by the Graduate School

Lawrence Martin
Dean of the Graduate School

Abstract of the Thesis

Physical Characteristics of Bering Sea Zooplankton and Their Use to Parameterize an Acoustic Scattering Model for Euphausiids

by

Joy Nicole Smith

Master of Science

in

Marine and Atmospheric Science

Stony Brook University

2010

Acoustic assessment of Bering Sea euphausiids and their predators can provide useful data for ecosystem studies if the acoustic scattering characteristics of these animals are known. The amount of acoustic energy that is scattered by different marine zooplankton taxa is strongly affected by the contrast of the animal's density (g) and sound speed (h) with the surrounding seawater. Density and sound speed contrast were measured in the Bering Sea during the summer of 2008 for several different zooplankton and nekton taxa including: euphausiids (*Thysanoessa inermis, Thysanoessa raschii,* and *Thysanoessa spinifera*), copepods, amphipods, chaetognaths, gastropods, fish larvae, jellyfish, and squid. Density contrast values varied between different taxa as well as between individual animals within the same species. Sound speed contrast was measured for monospecific groups of animals and differences were found among taxa. The range, mean, and standard deviation of g and h for all euphausiid species were: g = 1.001-1.041; 1.018 ± 0.009 and h = 0.990-1.017; 1.006 ± 0.008. Changes in the relationship between euphausiid material properties and animal length, seawater temperature, seawater density, and geographic location were also evaluated. Results suggest that environmental conditions at different sample locations led to significant differences in animal density and material properties.

Acoustic surveys monitor euphausiid populations in the Bering Sea because of their importance as prey walleye pollock. Various scattering models exist to convert acoustic survey data to numerical density estimates of euphausiids, but a target strength (TS) model specific to Bering Sea euphausiids did not exist. This study parameterized a distorted wave Borne approximation model using measured lengths and material properties (density contrast, g, and sound speed contrast, h) from live euphausiids. All model parameters (length, g, h, shape, orientation) were evaluated for their effect on TS estimates.

Table of Contents

List of Figures

List of Tables

Acknowledgments

This project was supported by the Alaska Fisheries Science Center, National Marine Fisheries Service, NOAA, and the North Pacific Research Board's Bering Sea Integrated Ecosystem Research Program. The captain, crew, and scientists aboard the NOAA ship *Oscar Dyson* provided excellent logistical support and sampling assistance. Abigail McCarthy helped us greatly with the set up and maintenance of the on board aquaria as well as with the trawl sampling operations. We acknowledge the taxonomic advice of Elaina Jorgensen (squid) and Claudia Mills (hydromedusae). We would like to thank Alex De Robertis and Neal Williamson for their comments and suggestions on this manuscript. The statements, findings, conclusions, and recommendations in this manuscript are those of the authors and do not necessarily reflect the views of NOAA or the U.S. Department of Commerce. This paper is BEST-BSIERP Publication #xxx, NPRB Publication #yyy, and Marine Sciences Research Center contribution #zzz.

CHAPTER 1

Material properties of euphausiids and other zooplankton from the Bering Sea

I. INTRODUCTION

Zooplankton form a key trophic link between primary producers and higher trophic level consumers in pelagic marine ecosystems (Springer and Roseneau, 1985; Brodeur *et al.*, 2002). Euphausiids, along with more variable contributions from calanoid copepods and juvenile walleye pollock, are the most important prey items for the walleye pollock (*Theragra chalcogramma*) stock on the Bering Sea shelf (Dagg *et al.*, 1984; Livingston, 1991; Cianelli *et al.*, 2004). Ecologically, walleye pollock are a keystone species (Springer, 1992) in the Bering Sea and are important prey for northern fur seals and other marine mammals, as well as for foraging fish and seabirds (Coyle *et al.*, 1992; Sinclair, 1994; Decker and Hunt, 1996). Economically, the pollock fishery is the largest U.S. fishery by mass and makes up over 40% of the global whitefish production (Ianelli *et al.*, 2008). Walleye pollock are broadly distributed throughout the North Pacific, with the largest concentrations found throughout the Eastern Bering Sea (Ianelli *et al.*, 2008). Acoustic surveys along with net trawls are regularly conducted to estimate the abundance and distribution of the walleye pollock population there (e.g., Honkalehto *et al.*, 2009). These survey data sets may also be used to identify and quantify the abundance of some zooplankton taxa.

Acoustic techniques allow scientists to observe the spatial and temporal variability in zooplankton distributions with a greater resolution and broader areal coverage than traditional net sampling. Acoustic surveys using multiple frequencies (e.g. 38, 120, and 200 kHz) have previously been applied to the study of zooplankton in the Bering Sea (Coyle and Pinchuk, 2002, Honkalehto *et al.*, 2002). However, in order for acoustic backscatter measurements to be used as a quantitative tool for studying these populations, it is necessary to have a well-constrained estimate of target strength (TS) to convert

acoustic energy into a particular biological metric (e.g. numerical density, animal taxon, biomass; Simmonds and MacLennan, 2005). TS estimates are available for many species including walleye pollock (Traynor, 1996), other commercially-important fish species (Simmonds and MacLennan, 2005), and Antarctic euphausiids (Demer and Conti, 2005), but such estimates do not exist for Bering Sea zooplankton. In the absence of direct measurements, TS can be estimated through the use of acoustic scattering models for zooplankton (see review by Foote and Stanton, 2000). TS is a function of the acoustic frequency and the size, shape, orientation, and material properties of the animal (Stanton and Chu, 2000; Chu *et al*., 2000; Warren *et al*., 2002). If more information is known about the physical characteristics of the target, then more accurate scattering model predictions will result in improved acoustic predictions of biological information (Stanton and Chu, 2000).

The two material properties most important to zooplankton scattering model predictions are *g*, the density contrast between a target and the surrounding seawater, and *h*, the sound speed contrast between a target and the surrounding seawater (Anderson, 1950). Along with animal length, the density and sound speed contrasts are particularly critical parameters for predicting scattering from crustacean zooplankton because these animals are modeled as weakly scattering fluid-like objects with material properties similar to that of the surrounding seawater. Small changes in these parameters can cause large changes in the predicted scattering from the animal (Stanton *et al*., 1994; Wiebe *et al.*, 1997; Stanton and Chu, 2000). Modeling by Chu *et al.* (2000) has predicted up to a 20 dB difference in TS for weakly scattering euphausiid-like zooplankton ($g = 1.0357$, $h = 1.0279$) with only a 2 - 4 % change in *g* and *h*. Relatively few studies have measured the material properties of specific zooplankton taxa. The available data show that *g* and *h* vary significantly among different types of zooplankton (Greenlaw and Johnson, 1982; Foote *et al.*, 1990; Chu and Wiebe, 2005; Warren and Smith, 2007), as well as within the same zooplankton taxon from individual to individual (Forman and Warren, 2009), between geographic regions, and through time both seasonally and as the organisms age (Hagen *et al.*, 1996; Køgeler *et al.*, 1987). For each geographical area under study, it would be ideal to measure parameters such as animal length and material properties of

living specimens from different zooplankton groups for use in these scattering models.

This study measured the physical characteristics and material properties of several types of zooplankton from the Bering Sea during the summer of 2008. Animals were grouped into different taxonomic categories for analysis of their size and material properties and the ranges in *g* and *h* values for each zooplankton taxon were measured. These taxa included *Thysanoessa raschii* and *Thysanoessa inermis*, the two euphausiid species that dominate zooplankton biomass in the Bering Sea (Smith, 1991), along with a less dominant euphausiid species, *Thysanoessa spinifera.* Several other zooplankton taxa were collected and studied including: copepods (*Neocalanus sp.*), amphipods (*Themisto libellula*), chaetognaths (*Sagitta sp.*), gastropods (*Clione limacina*), larval fish (*Theragra chalcogramma*), and jellyfish (*Chrysaora melanaster* and an unidentified species, possibly *Polyorchis penicillatus*). One nektonic taxon, a squid of the family Gonatidae (species undetermined), was also collected and the material properties of some of their body parts were measured. Although squid are not zooplankton, they are often present in the water column and can be significant scatterers of acoustic energy (Greenblatt, 1981; Brierley and Watkins, 1996). Material properties of euphausiids and copepods were compared to previous measurements of these zooplankton in the Barents Sea and elsewhere (Greenlaw and Johnson, 1982; Køgeler *et al.*, 1987; Foote, 1990; Chu and Wiebe, 2005). We also examined the influence on *g* from animal length, environmental factors (such as seawater temperature and salinity), geographic location, and food availability as measured by fluorescence.

II. METHODS

A. Zooplankton collection and husbandry

Live zooplankton were collected using a Methot trawl (MT) at nine stations sampled during an acoustic-trawl pollock survey in the Bering Sea aboard the NOAA ship *Oscar Dyson* from 20 June to 09 July 2008 (Honkalehto *et al*., 2009; Fig. 1). The Methot trawl is a rigid frame trawl with a mouth area of 5 m^2, 2 mm by 3 mm oval mesh in the body of the net, and 1 mm mesh in the hard codend (Methot, 1986). In order to obtain live specimens in a minimally-stressed, healthy condition and to maximize the

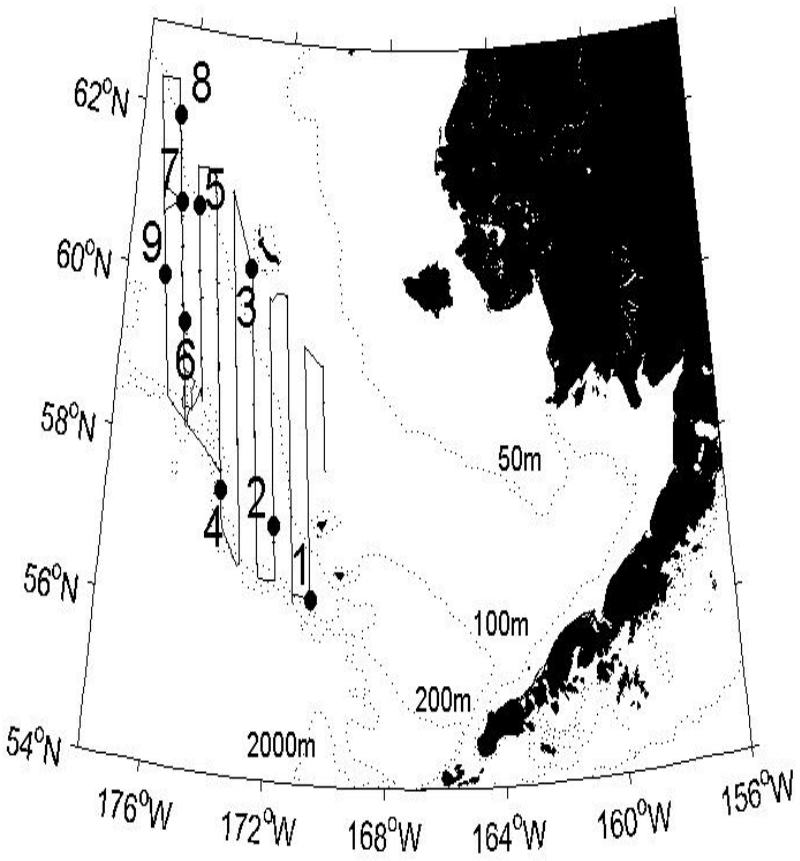

Figure 1. Cruise trackline (solid line) of the NOAA Ship *Oscar Dyson* from 20 June to 09 July 2008. Methot trawl locations are identified (filled circles) and numbered. Bathymetry contours (dotted lines) are shown for 50, 100, 200, and 2000 m.

number of animals captured, short duration (average 4.5 min) and shallow (average maximum depth 12.1 m) hauls were conducted at night when zooplankton aggregations in surface waters were expected to be abundant. Upon retrieval of the net, the contents of the codend from each tow were immediately transferred to a large container (~100 L) containing surface seawater. The taxa collected in the Methot trawls included euphausiids, copepods, amphipods, chaetognaths, gastropods, fish larvae, and jellyfish. All zooplankton (or a subset consisting of the most healthy animals depending on the number of animals caught) were then sorted by hand into smaller containers (2 or 34 L)

by taxon. They were kept alive until measurements of the physical characteristics and material properties could be made. Animal density measurements were typically made within 6 hours (and all measurements were made within 48 hours) of being collected.

In addition to the Methot trawl sampling, animals collected in large mid-water trawls conducted as part of the pollock survey (an Aleutian Wing trawl with a mouth area of about 650 m^2; Honkalehto *et al*., 2002) were also used in this study. While some jellyfish were caught in the Methot trawl, large jellyfish (e.g., *Chrysaora melanaster* with bell diameters ranging from 15 to 24 cm) and squid specimens were caught in the mid-water trawl nets, along with pollock and other large nekton. Both the large jellyfish and squid specimens were alive and moving when brought onboard the vessel and were placed in containers (~10 L) of seawater. Unlike the zooplankton captured by the Methot trawl, these animals were likely traumatized or damaged by the net tow collection process. Due to the size of these animals, material property measurements were made on excised parts.

Measurements were taken for a variable number of animals from each taxon depending on the number of animals caught and sorted from each tow. For example, a typical tow contained several hundred to thousands of euphausiids and copepods, while ten to fifty animals from the other taxa were collected. Measurements on individual animals included species identification (when possible), animal length and width, and animal density (ρ). Measurements on groups of animals from each taxon included sound speed contrast (h). Animals used for the density measurements were separated by taxon and placed into large (34 L) and small (2 L) aerated plastic tanks containing pumped, ambient surface seawater (average temperature 4 °C) in a controlled environment room (air temperature ranging from 2.7 - 7.2 °C). The large containers held euphausiids and copepods, while the small containers held amphipods, chaetognaths, gastropods, fish larvae, and jellyfish. Animals used in the sound speed experiments were placed in small (2 L) tanks with ambient surface seawater and were then transferred into the chamber used for the h measurements shortly after the sorting process was completed. The temperature and salinity of the surrounding seawater in the tanks were recorded for each experiment.

B. Length measurements

Animal lengths were measured for a subsample of animals collected by each Methot trawl. Every animal that had its density measured also had its length recorded. Organisms from a separate subset of animals from each MT had both their lengths and widths measured. Euphausiid lengths were measured from the front of the eye to the end of the telson with the animal positioned as straight as possible. Lengths measured for other zooplankton taxa were total lengths in which the animal was positioned as a straight as possible. Length and width are input variables used in many target strength models (Stanton and Chu, 2000). The relationship between animal length and g was evaluated through linear regressions for those taxa in which g was measured for the entire animal (as opposed to pieces of the animal) and there were a sufficient number of animals collected.

C. Material properties measurements

1. Density

The density (ρ) of individual animals from each taxon was measured and the density of the surrounding seawater was calculated from the temperature and salinity measurements. These values were then used to calculate the density contrast (g). Animal density was measured for the following: euphausiids, copepods, amphipods, chaetognaths, gastropods, fish larvae, jellyfish and squid body parts. Density measurements for most taxa were made on live organisms, so their movement had to be suppressed in order to accurately monitor any changes in buoyancy. Individual zooplankton were placed in a small container holding approximately 50 ml of seawater and 1 drop of clove oil until they stopped moving. Density measurements for fish larvae and most jellyfish were not conducted on live animals; however, the measurements were taken shortly after their death. Fish larvae typically did not survive the Methot trawl, while large jellyfish (*Chrysoara melanaster*) had to be cut into small pieces in order to fit into the equipment used to measure animal density. For squid, separate density measurements were recorded for different parts of the body (mantle, pen, beak) after each part was removed from the rest of itself. Beaks were stored in seawater while the pens and mantle pieces were frozen. The density of all three body parts of the squid were

measured separately in the laboratory after the cruise. In the cases where live animals of a taxon were not measured, we assume that any changes in density as a result of decomposition or time elapsed between capture and measurement were negligible (except where noted for the squid specimens).

Two different methods were used to measure the density of an animal: the titration method onboard the ship and the pipette method on land. The titration method (Warren and Smith, 2007) for all density measurements, except those of squid material, involved placing the animal in a beaker containing a known volume of ambient sea water (V_{sw}). A solution of higher-salinity seawater was created by dissolving Instant Ocean® (Aquarium Systems, Inc., Mentor, OH). into ambient seawater. This saltier water was then titrated into the beaker until the buoyancy of the animal was altered and the animal began to rise. The volume of the hypersaline solution required to make the animal float was recorded (V_{hs}). For some individual animals that were positively buoyant, fresh water was titrated into the container until the buoyancy of the animal changed and the animal began to sink. Prior to each measurement, the temperature, salinity, and conductivity of the water were recorded (YSI 65, YSI Incorporated). The temperature and salinity of the ambient, fresh, and hypersaline seawater solutions were used to calculate the solution density using the CSIRO MATLAB Seawater Library. With the information collected, the density of the individual animal was calculated based on the following equation:

$$\rho_{animal} = \frac{((\rho_{sw} V_{sw}) + (\rho_{hs} V_{hs}))}{(V_{sw} + V_{hs})} \quad , \qquad (1)$$

where ρ_{sw} is the density of seawater (g ml^{-1}), V_{sw} is the volume of seawater water used initially to hold the organism (ml), ρ_{hs} is the density of the solution (g ml^{-1}), and V_{hs} is the volume of solution used in the titration (ml).

Because the titration method involved adding a saltier solution to the seawater surrounding the animal, it is possible that the resulting osmotic pressure could have altered the density of the animal. We observed that a change in the buoyancy occurred over the course of several minutes if the animal was allowed to remain in the solution after the saltier solution had been added. In this study, the measurement needed for

estimation of animal density using the titration method was completed within approximately 30 seconds of the saltier solution being added, which we believe minimized the chance of osmotic adjustment by the animal. In addition, the titration method was performed multiple times on each animal; the density measurements were similar between iterations and had a mean percent difference of 0.41 %. This small mean percent difference, with no systematic change in animal density after repeated iterations, suggests that there was no bias due to osmotic effects in density measurements using the titration method. Another possible source of error with this method is that seawater bound to the animal by surface tension will bias the measurement towards unity, since the titration method measures the density of the animal along with any seawater that is attached to the animal by surface tension. This factor will increase in importance as animal volume decreases and thus is most likely to impact the smallest animals we measured, the copepods. However, other studies have used similar density measurement methods on even smaller copepods than those in this study (Køgeler *et al.*, 1987; Greenlaw and Johnson, 1982; Greenlaw, 1977).

Once the density of the animal was measured, *g*, the ratio of the animal density to the density of the seawater, was calculated using the following equation:

$$g_{animal} = \frac{\rho_{animal}}{\rho_{sw}} \quad . \tag{2}$$

The maximum potential error that can result from calculating animal density has previously been estimated for material property measurements of different zooplankton species collected from Antarctic waters (Chu and Wiebe, 2005). The maximum potential error associated with the equation used to calculate the density of Bering Sea euphausiids (Eq. 1) was also estimated with the equation:

$$\delta\rho_{animal} = [(V_{sw}\frac{\rho_{sw}}{(V_{sw}+V_{hs})})(\frac{\delta V_{sw}}{V_{sw}}+\frac{\delta\rho_{sw}}{\rho_{sw}}+(\frac{(\delta V_{sw}+\delta V_{hs})}{(V_{sw}+V_{hs})}))]$$

$$+[(V_{hs}\frac{\rho_{hs}}{(V_{sw}+V_{hs})})(\frac{\delta V_{hs}}{V_{hs}}+\frac{\delta\rho_{hs}}{\rho_{hs}}+(\frac{(\delta V_{sw}+\delta V_{hs})}{(V_{sw}+V_{hs})}))] \quad . \tag{3}$$

The estimated uncertainty of the instrumentation for each parameter was $\delta\rho_{sw} = 4\text{x}10^{-5}$ g

ml^{-1}, $\delta\rho_{hs} = 4x10^{-5}$ g ml^{-1}, $\delta V_{sw} = 0.05$ ml and $\delta V_{hs} = 0.05$ ml. The maximum potential error for the animal density was $\delta\rho_{animal} = 0.0129$. As the name implies, the maximum potential error gives the greatest possible value of error, however this value is likely to be an overestimation if the uncertainty from the instrumentation is independent and random, as it is in this study. Therefore, a more realistic estimate of the combined uncertainty can be made through quadrature addition. This error analysis technique is based on the principle that measurements from two independent instruments (for example, x and y) will have a normal distribution (thus, an associated σ_x and σ_y) around their true value (X and Y). The associated error from summing x and y would then be governed by statistical rules and be described by $\sqrt{[(\sigma_x)^2+(\sigma_y)^2]}$ (Taylor, 1982). Applying the quadrature technique to Eq. 1, the error estimated through quadrature was calculated using Eq. 4:

$$\delta\rho_{animal} = \rho_{animal} * \sqrt{\left(\frac{\rho_{sw}}{(V_{sw}\rho_{sw}+V_{hs}\rho_{hs})}-\frac{1}{(V_{sw}+V_{hs})}\right)^2 \delta V_{sw}^2+\left(\frac{V_{sw}}{(V_{sw}\rho_{sw}+V_{hs}\rho_{hs})}\right)^2 \delta\rho_{sw}^2}$$

$$\sqrt{+\left(\frac{\rho_{hs}}{(V_{sw}\rho_{sw}+V_{hs}\rho_{hs})}-\frac{1}{(V_{sw}+V_{hs})}\right)^2 \delta V_{hs}^2+\left(\frac{V_{hs}}{(V_{sw}\rho_{sw}+V_{hs}\rho_{hs})}\right)^2 \delta\rho_{hs}^2} \quad . \qquad (4)$$

The estimated uncertainty for each parameter remained the same for both error analysis equations, ($\delta\rho_{sw} = 4x10^{-5}$ g ml^{-1}, $\delta\rho_{hs} = 4x10^{-5}$ g ml^{-1}, $\delta V_{sw} = 0.05$ ml and $\delta V_{hs} = 0.05$ ml), however the calculated error through quadrature was approximately two orders of magnitude lower than the error calculated using the maximum potential error equation and had a value of $\delta\rho_{animal\_quad} = 1.1721x10^{-4}$. Since the error estimated through quadrature was small, fluctuations in the *g* measurements were likely the result of variability from animal to animal instead of error from the instrumentation.

The titration method was used to measure the density of squid beak pieces, but instead of a hypersaline solution being used as the titrant, glycerine ($\rho = 1.173$ g ml^{-1}) was used since the beaks were substantially more dense than the hypersaline solution. Squid beaks were excised from the surrounding tissue, stored in seawater, and brought back to the laboratory. There was no visible deterioration or dissolution of the squid beaks from when they were collected and when they were measured. The jaw was divided into top

and bottom portions and the density of each piece was measured. Two measurements were taken for each squid beak piece and the mean percent difference between the trials was 0.46 %. We had hoped to also measure the density of the squid pen in addition to the beak and mantle; however, the pens deteriorated even more than the squid mantle by the time the density measurements were taken, so no results for the pens are reported.

The pipette method (Warren and Smith, 2007; Forman and Warren, 2009) was used to measure squid mantle density, since this material was too dense to be properly measured using the titration method. Squid mantles were cut into multiple pieces which were frozen, transferred back to the laboratory, then thawed. The mass of a piece of mantle was measured after excess water had been removed and then the tissue was placed in a graduated cylinder containing a known volume of seawater. The amount of water displaced by the mantle was extracted and weighed. The density of the mantle was calculated using the following equation:

$$\rho_{animal} = \frac{m_a}{\left(\frac{m_d}{\rho_{sw}}\right)} \quad , \tag{5}$$

where m_a is the mass of the animal (g); m_d is the mass of water displaced by the organism (g), and ρ_{sw} is the density of the seawater (g ml^{-1}). The density of each mantle piece was measured twice and the mean percent difference between trials was 1.55%. Similar to the titration method, g was calculated using Eq. 2. As the squid mantle measurements were made on frozen and thawed samples, the mantle was slightly deteriorated by the time the measurement was taken. Considering the interest in material properties of squid (Kang *et al.*, 2004), we present these data with the caveat that our measurements may be biased due to degradation of the tissue.

2. Sound speed

The sound speed contrast (h) was measured for euphausiids, copepods, jellyfish, amphipods, and gastropods. Animals were placed in a small chamber (PVC t-tube), with a volume of either 26 or 84 ml depending on the size and number of the animals being measured. Two 500 kHz transducers (one transmitter, one receiver) were clamped on

either end of the containers. The time it took for a sound wave to travel from one end of the container to the other was recorded when the compartment contained only seawater and when it was full of a mixture of zooplankton and seawater. Knowing the difference in travel time, along with the container volume and zooplankton volume, *h* (the ratio of sound speed through zooplankton tissue (c_a) compared to sound speed through seawater (c_{sw})) was calculated with the following equation:

$$h = \frac{c_a}{c_{sw}} = 1 + \frac{\Delta t}{(\Phi t_d)} \quad , \tag{6}$$

where Δt is the time (s) it takes for sound to travel through animals from transducer to receiver, Φ is the volume fraction ($\Phi = V_{tube}/V_{animal}$ where V_{tube} is the volume (ml) of the PVC-tube chamber and V_{animal} is the volume (ml) of the zooplankton), and t_d is the travel time (s) of sound from transducer to receiver with an empty chamber (Greenlaw and Johnson, 1982; Køgeler *et al.,* 1987; Chu *et al.,* 2000; Chu and Wiebe, 2005; Warren and Smith, 2007). The animal volume (V_{animal}) was measured using the displacement method in which the a known volume of water filled the chamber, animals were then placed inside the chamber, and the volume of water displaced by the animals was measured. The maximum potential error attributed to the instrumentation was estimated from Eq. 6 using the following:

$$\delta h_{max} = h\left(\frac{\delta \Delta t}{\Delta t} + \frac{\delta \Phi}{\Phi} + \frac{\delta t_d}{t_d}\right) \quad , \tag{7}$$

while the error estimated through quadrature was calculated with:

$$\delta h_{quad} = \sqrt{\left(\frac{1}{(\Phi t_d)}\right)^2 \delta \Delta t^2 + \left(\frac{-\Delta t}{(t_d \Phi^2)}\right)^2 \delta \Phi^2 + \left(\frac{-\Delta t}{(\Phi t_d^2)}\right)^2 \delta t_d^2} \quad . \tag{8}$$

The uncertainties corresponding to each variable were estimated as δΦ = 0.04, δΔt = 5.44×10^{-8}s, and $\delta t_d = 1.62 \times 10^{-7}$s. The volume fraction uncertainty was estimated using the uncertainty of the graduated cylinder used to measure the volumes of the animals and chamber (0.5 ml). The typical volume of animals in the chamber was 20 ml which results in an uncertainty in the volume fraction of 0.04. The maximum potential error calculated

for all zooplankton groups was $\delta h_{max} = 0.1922$ while the error calculated through quadrature was $\delta h_{quad} = 1.5 \times 10^{-3}$. Similar to the error analysis used for *g*, the maximum potential error calculated for *h* was likely to be an overestimate of the true error since the uncertainties of each parameter were independent and random. Thus, a more reasonable estimate of our measurement uncertainty was obtained from the quadrature method using Eq. 8.

The criteria for determining which zooplankton groups would be measured for *h* depended on the volume of each zooplankton group caught in the net tow. The volume of zooplankton had to be enough to fill (or nearly fill) the measurement chamber in order to get an accurate measurement of sound speed contrast. The *h* measurements were likely biased minimally (towards unity) considering the difficulty in entirely removing excess water from around the animals and the difficulty in completely filling the chamber with animals (i.e., Φ is always less than 1).

D. Other parameters measured

1. Biomass Density

The wet weight of all zooplankton collected by each Methot trawl (MT) was measured and the total volume of water filtered by the MT was calculated by multiplying the area of the opening of the MT and the distance sampled. Both the wet weight and total volume filtered were used to calculate zooplankton biomass density (g m^{-3}).

2. Environmental variables

Animal density contrast is a function of both the density of the animal and the density of the surrounding seawater. Since both temperature and density vary vertically and horizontally (e.g., across frontal regions) in the ocean, changes in *g* as a function of these parameters were examined. The average water temperature of the containers holding zooplankton was 4 °C. Several experiments were conducted in which this temperature was manipulated to see if it affected the animal density contrast (*g*). Water temperature was cooled by placing the container with the live animals in an ice bath. Subsequently, temperatures warmed naturally through time as the water adjusted to the surrounding air temperature. Water temperatures ranged from 0.6 °C to 6.3 °C, which lies within the range of water temperatures that zooplankton may experience throughout

the year within the Bering Sea (Coyle *et al.*, 2008). Experiments in which water temperature was manipulated were conducted only for euphausiids since they were the main zooplankton group of interest and most common animal in the Methot trawl catches. We also recorded the changes that occurred in the salinity and density of the water the euphausiids were kept in over the course of the experiments. The influence of ambient water conditions (temperature, salinity, and density) on *g* was evaluated.

Chl-a fluorescence data were collected from a WETStar (WETLabs) sensor on a Conductivity-Temperature-Depth (CTD) rosette deployed at multiple stations during the cruise. Seven of the MT locations (MT01, MT02, MT04, MT05, MT07, MT08, MT09, Fig. 1) had CTD profiles conducted either immediately before or after the MT, while two MT locations (MT03, MT06) did not. Chlorophyll-a (chl-a) concentration (mg m^{-3}, based on a factory calibration of chl-a fluorescence from the WETStar sensor) was used as a proxy of zooplankton prey (phytoplankton) at each location. Pearson correlations were computed between euphausiid *g* and the chl-a concentration at the water depth from which the zooplankton were collected. Pearson correlations were also computed between *g* and the integrated chl-a over the entire water column.

3. Statistical analysis

Since the variables that potentially have an effect on *g* may also be inter-related, a principal component analysis was performed in order to reduce the variables with redundant behavior into several factors which account for the variance in the observed data. The relationships among variables and between groups of variables and *g* were also explored. Secondly, a linear regression was performed to evaluate the effect of length on *g*. Finally, factorial ANOVAs were used to determine whether or not particular variables affected *g* by themselves or whether or not those variables interacted with one another to simultaneously affect *g*.

III. RESULTS

Total zooplankton biomass density in Methot catches varied from 2.5 g m^{-3} (MT04, the largest value observed) to 0.03 g m^{-3} and 0.05 g m^{-3} (MT06 and MT07, respectively) and were dominated by euphausiids, copepods, and parts of gelatinous

zooplankton. Not all taxa were collected at each station; of all the zooplankton taxa that were collected and measured (Fig. 2) euphausiids were most common and present in all MTs.

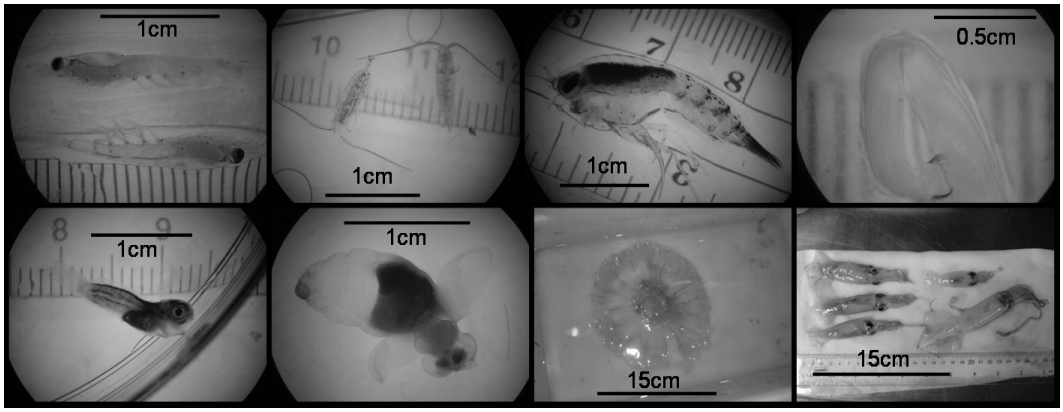

Fig. 2. Representative photographs of taxa collected and measured for their material properties. Top row (from left to right): euphausiid, copepod, amphipod, chaetognath. Bottom row (from left to right): fish larvae, gastropod, jellyfish, squid.

However, the relative abundance of the three euphausiid species differed with location (Fig. 3). The two dominant euphausiid species were *T. inermis* and *T. raschii*, while *T. spinifera* were only present in MT04.

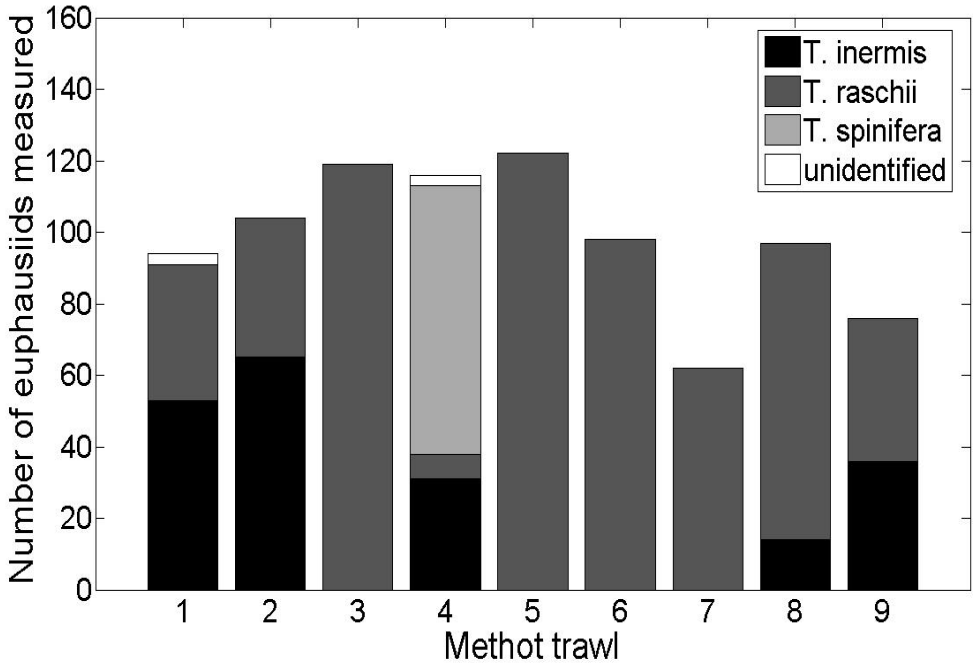

Fig.3. Species composition of euphausiids caught in Methot trawls that were measured for their physical (length) or material (*g*, *h*) properties.

The average and standard deviation of *g* and animal length for euphausiids were calculated for each species; whereas the average and standard deviation of *h* were calculated for each MT (Table 1).

Table 1. Mean and standard deviation (sd) of material properties, physical features, and environmental variables for euphausiids at each MT. Density contrast (g) values are presented for all euphausiid species combined as well as for each individual species. The sd for all water density measurements was negligible (< 0.001).

MT	**Taxonomic group**	**Animal length (mm)**		**Density contrast**		**Sound speed contrast *(h)***	**Temperature (°C)**	**Salinity (ppt)**	**Water density (g ml^{-1})**
		length	**n**	***g***	**n**				
MT01	all euphausiids	19.6 ± 9.1	94	1.005 ± 0.002	61	1.008	4.4 ± 2.4	32.1 ± 0.1	1.025
	T. inermis	20.1 ± 2.5	53	1.006 ± 0.002	29				
	T. raschii	18.7 ± 1.8	41	1.004 ± 0.002	15				
MT02	all euphausiids	20.4 ± 2.5	104	1.007 ± 0.005	54	1.002	5.5 ± 0.5	32.9 ± 0.5	1.026
	T. inermis	20.3 ± 2.6	65	1.007 ± 0.005	38				
	T. raschii	20.6 ± 2.1	39	1.009 ± 0.005	16				
MT03	all euphausiids	15.3 ± 1.7	117	1.019 ± 0.007	67	0.996	4.7 ± 0.8	30.4 ± 0.4	1.024
	T. raschii	15.3 ±1.7	117	1.019 ± 0.007	67				
MT04	all euphausiids	20.0 ± 3.3	118	1.017 ± 0.007	58	1.006	4.0 ± 1.3	33.4 ± 0.9	1.026
	T. inermis	19.4 ± 1.3	31	1.018 ± 0.004	20				
	T. raschii	19.0 ± 1.0	8	1.016 ± 0.003	3				
	T. spinifera	20.5 ± 2.4	76	1.017 ± 0.005	32				
MT05	all euphausiids	16.3 ± 1.3	122	1.024 ± 0.006	72	1.012	4.1 ± 2.0	33.0 ± 1.2	1.026
	T. raschii	16.3 ± 1.3	122	1.024 ± 0.006	72				
MT06	all euphausiids	17.5 ± 1.4	98	1.023 ± 0.006	48	n/a	3.9 ± 2.6	33.2 ± 1.4	1.026
	T. raschii	17.5 ± 1.4	98	1.023 ± 0.006	48				
MT07	all euphausiids	16.9 ± 1.1	62	1.027 ± 0.003	12	0.990	4.9 ± 0.0	32.7 ± 0.0	1.027
	T. raschii	16.9 ± 1.1	62	1.027 ± 0.003	12				
MT08	all euphausiids	19.1 ± 3.0	98	1.022 ± 0.008	48	1.006	3.3 ± 2.4	34.5 ± 0.3	1.027
	T. inermis	17.9 ± 2.2	14	1.018 ± 0.006	10				
	T. raschii	19.4 ± 3.1	83	1.024 ± 0.008	38				
MT09	all euphausiids	19.0 ± 2.3	77	1.019 ± 0.006	27	1.014	2.6 ± 2.2	32.1 ± 0.4	1.026
	T. inermis	18.8 ± 1.9	36	1.016 ± 0.004	17				
	T. raschii	19.3 ± 2.8	41	1.024 ± 0.005	10				

Environmental parameters measured for the ambient water the euphausiids were kept in during the experiments (a function of both natural environment and experimental manipulation; Table 1), and for the water column at each location were also reported (Table 2). These data are representative of environmental conditions and material properties for euphausiids during summer in the Bering Sea.

Table 2. Average water column properties for MT stations, based on nearby CTD casts. No data were available for MT03 and MT06.

Location	**Top 5 m water temperature (ºC)**	**Average water column temperature (ºC)**	**Average water column salinity (ppt)**	**Average water column σ_t (kg m^{-3})**	**Average water column chlorophyll-a (mg m^{-3})**
MT01	5.8	3.8	32.3	25.9	4.0
MT02	5.4	3.4	32.4	26.1	3.1
MT04	6.3	3.5	32.8	25.7	6.0
MT05	5.5	-0.4	32.0	26.1	3.6
MT07	5.3	0.3	32.1	26.0	1.8
MT08	5.7	0.1	32.1	26.0	3.0
MT09	3.9	0.8	32.4	26.3	1.7

A. Length distributions

Animal lengths varied both within and between different taxa (Table 3). There were a sufficient number of specimens to determine the length distribution for euphausiids, copepods, and amphipods. The length distributions of euphausiids (for all species combined and each separate species) were roughly similar, with smaller animals being more abundant than larger animals (Fig. 4, Table 3). The mean length (mm) and standard deviation (sd) for all euphausiid species combined as well as for each species was as follows: all (18.2 ± 5.0), *T. inermis* (19.2 ± 2.4), *T. raschii* (17.2 ± 2.5), and *T. spinifera* (20.6 ± 2.4). The length distribution of copepods was also unimodal with a mean and standard deviation of 8 ± 0.45 mm, although the range in lengths was much

narrower compared to euphausiids.

Table 3. Range, mean, and standard deviation (sd) of animal length, density contrast (*g*), and sound speed contrast (*h*) for different zooplankton taxa; regardless of location. The number of animals measured (n) for *g* from each taxon is also presented along with the number of animal groups (nn) for which *h* was measured. Data presented for *Chrysaora melanaster* is from pieces of their bell, not the whole animal.

Zooplankton taxon	n	**Animal length (mm)**		**Density contrast (*g*)**		**nn**	**Sound speed contrast (*h*)**	
		Range	**Mean ± sd**	**Range**	**Mean ± sd**		**Range**	**Mean ± sd**
Euphausiids (all species)	448	12 to 27	18.2 ± 5.0	1.001 to 1.041	1.018 ± 0.009	12	0.990 to 1.017	1.006 ± 0.008
T. inermis	114	15 to 26	19.2 ± 2.4	1.001 to 1.027	1.011 ± 0.007	n/a	n/a	n/a
T. raschii	282	12 to 27	17.2 ± 2.5	1.001 to 1.041	1.021 ± 0.008	n/a	n/a	n/a
T. spinifera	32	17 to 27	20.6 ± 2.4	1.004 to 1.029	1.017 ± 0.005	n/a	n/a	n/a
Copepods	90	7 to 9	8.0 ± 0.45	0.995 to 1.015	1.005 ± 0.006	3	1.003 to 1.010	1.007± 0.004
Amphipods (all)	66	8 to 32	21.3 ± 8.3	1.001 to 1.029	1.010 ± 0.006	n/a	n/a	n/a
Small (<20 mm)	22	8 to 14	10.0 ± 1.7	1.001 to 1.009	1.005 ± 0.002	n/a	n/a	n/a
Large (>20 mm)	44	23 to 32	26.9 ± 2.4	1.002 to 1.029	1.013 ± 0.006	3	0.990 to 1.007	1.001 ± 0.009
Chaetognaths	14	13 to 35	25.6 ± 6.4	1.007 to 1.026	1.014 ± 0.007	n/a	n/a	n/a
Gastropods	17	9 to 23	14.9 ± 4.1	1.008 to 1.031	1.016 ± 0.006	1	n/a	1.008 ± 0.0
Fish larvae	15	20 to 33	23.8 ± 3.3	1.008 to 1.039	1.023 ± 0.008	n/a	n/a	n/a
Jellyfish (all)	40	20 to 95	49.0 ± 25.3	1.001 to 1.006	1.003 ± 0.001	n/a	n/a	n/a
Chrysaora melanaster	36	35 to 95	53.0 ± 28.0	1.001 to 1.006	1.003 ± 0.001	8	0.996to 1.007	1.002 ± 0.004
unidentified	4	21 to 31	24.0 ± 4.5	1.004 to 1.005	1.005 ± 0.001	n/a	n/a	n/a
Squid beak	30	25 to 17	5.0± 3.1	1.125 to 1.180	1.149 ± 0.013	2	1.010	1.010 ± 0.0

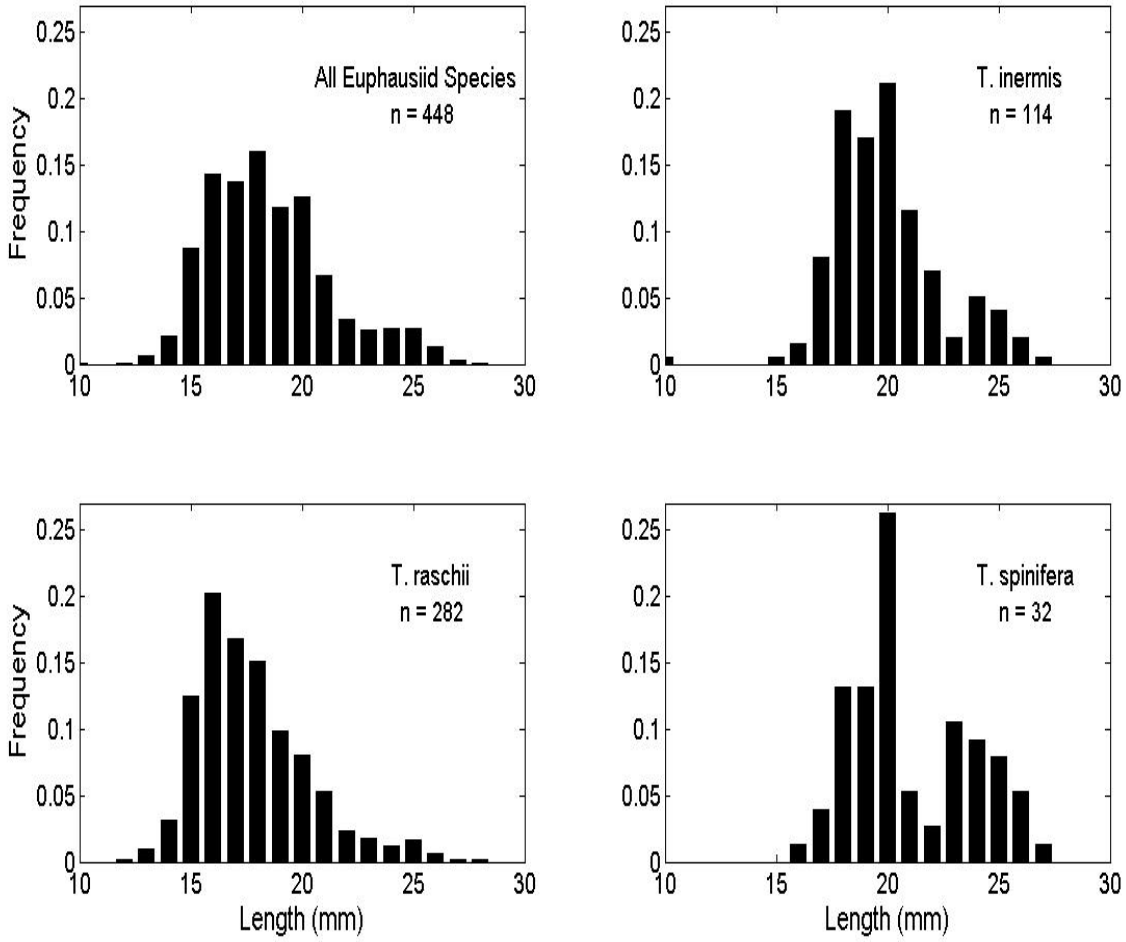

Fig.4. Length-frequency distributions for all euphausiids (upper left), T. inermis (upper right), T. raschii (lower left), and T. spinifera (lower right).

The length distribution of amphipods was bimodal. There were two size classes of amphipods: small (<20 mm) and large (>20 mm). Amphipods were found only in MT05 and MT08. With the exception of one animal, all of the small amphipods were collected from MT05 while large amphipods were collected at both MT05 and MT08. The bell diameter of the larger jellyfish species (*Chrysaora melanaster*) ranged from 150 to 240 mm with a thickness of 15 to 30 mm. They were drastically larger than the smaller, unidentified jellyfish (a bell-shaped hydromedusae) which had a bell diameter ranging in length from 20 to 31 mm with a bell thickness ranging from 5 to 9 mm.

B. Density

The density contrast varied among and within the different taxa (Fig. 5). A more detailed examination of the density contrast results for each taxon is presented below.

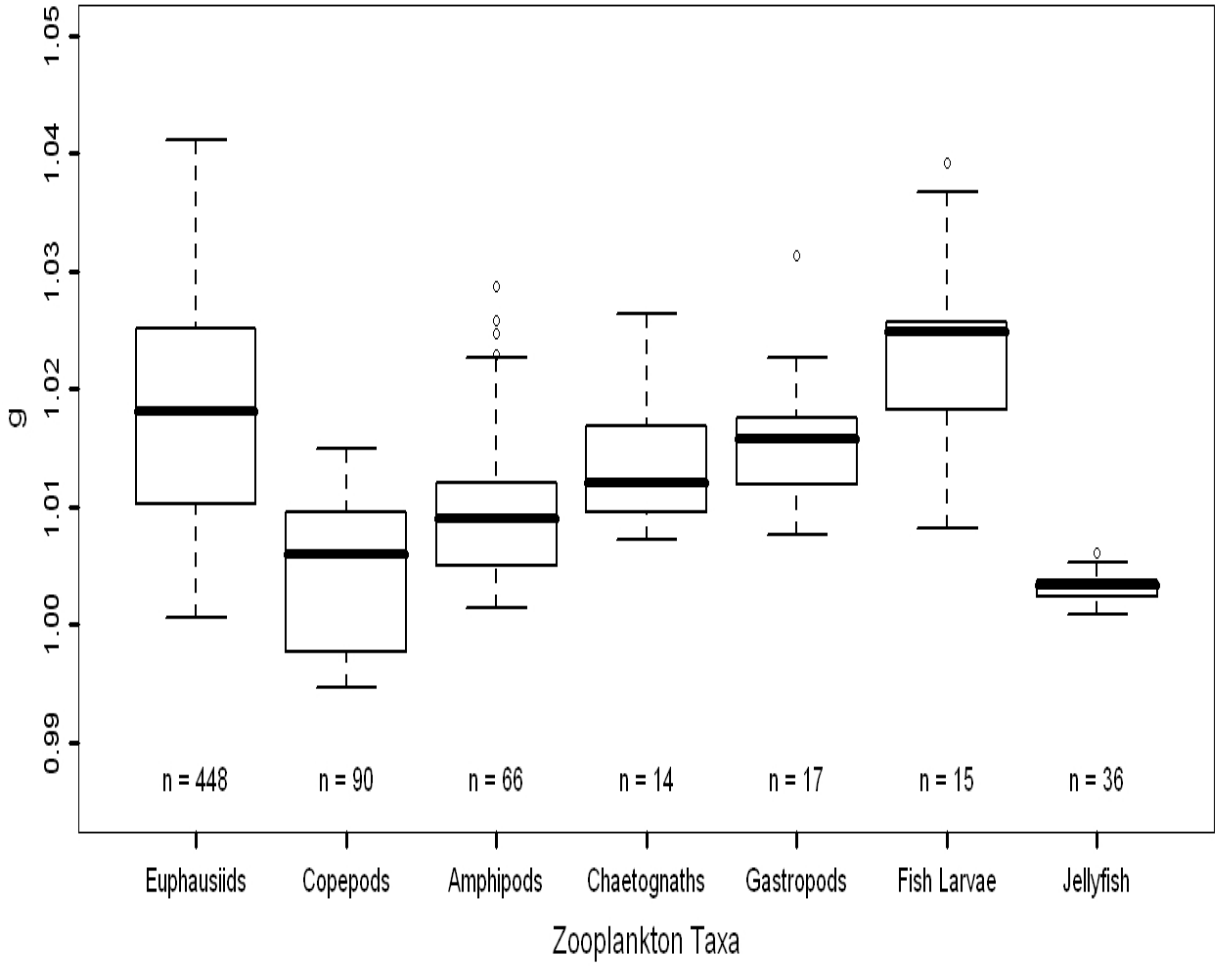

Fig.5. Density contrast of each zooplankton taxon. The lower line of the box represents the 1st quartile, the thick black line is the median, and the upper line of the box is the 3rd quartile while the whiskers are the maximum and minimum values. Circles represent outliers. The zooplankton taxa are all fluid-like and subsequently have lower values of *g*. Euphausiids have the largest range in *g* values while jellyfish (data from two species combined) have the smallest range in *g* values.

1. Euphausiids

Euphausiids were collected at all MT stations and the densities of 448 euphausiids were measured. As a group (all species), *g* ranged from 1.001 to 1.041 with a mean and sd of 1.018 ± 0.009 (Table 3). Pairwise scatter plots suggest a positive relationship between location (MT) and both *g* and the animal density for all euphausiids: both *g* and animal density increased in samples taken further to the west (Fig. 1, Fig. 6).

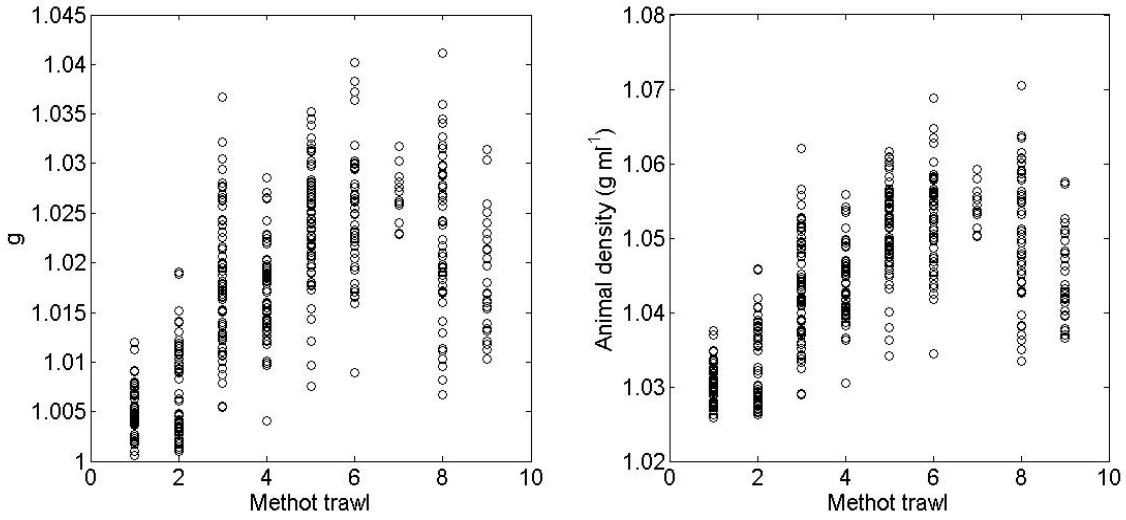

Fig.6. Pairwise scatterplots of *g* and animal density as a function of location for all euphausiids.

Similarly, we also examined the effects of temperature, salinity, and density of the water in which the animals were kept during the experiments on *g* (Table 1, Fig. 7); however, the relationships were weak for these variables. A principal component analysis (PCA) examined variation among these explanatory variables: MT, species, animal length, temperature, salinity, and water density. The PCA was conducted using only euphausiids with data for all variables, thus only 429 animals were used. The components were orthogonally rotated so correlations between the variables and the components could be more easily interpreted. The results indicated that PC1, PC2, and PC3 explained 39%, 23%, and 17% respectively (total 79 %) of the total variance. The major loadings on each primary component varied: PC1 (location (MT), salinity (ppt), and water density (g ml^{-1})), PC2 (location, temperature (°C), and animal length (mm)), and PC3 (species). These results suggest that spatial location and correlated changes in physical water

properties (density, salinity, and temperature) were responsible for most of the variance among explanatory variables, while animal length and species had measurable but weaker contributions.

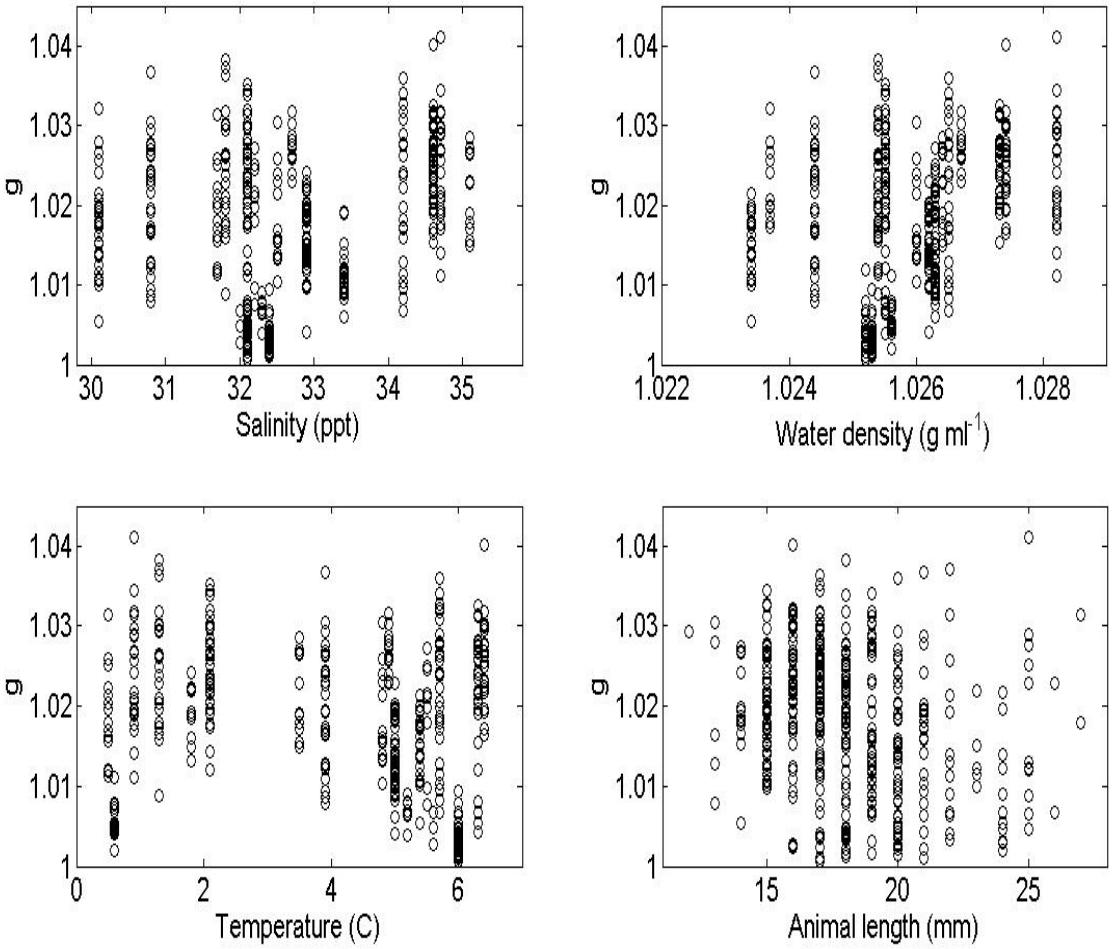

Fig.7. Pairwise scatter plots for ambient salinity, water density, temperature, and animal length against g. Location, salinity, and water density are components of PC1 and location, temperature and animal length are components of PC2. Although the relationship is weak, as PC1 increases so does g. On the contrary, as PC2 increases, *g* decreases.

Average *g* was slightly different among species (Table 3), but the uneven distribution of species by station (Fig. 3) makes it difficult to separate species effect from that of location. There was a similar trend in changes in *g* with location for both *T.*

inermis and *T. raschii,* the euphausiid species found at more than one station (Fig. 8).

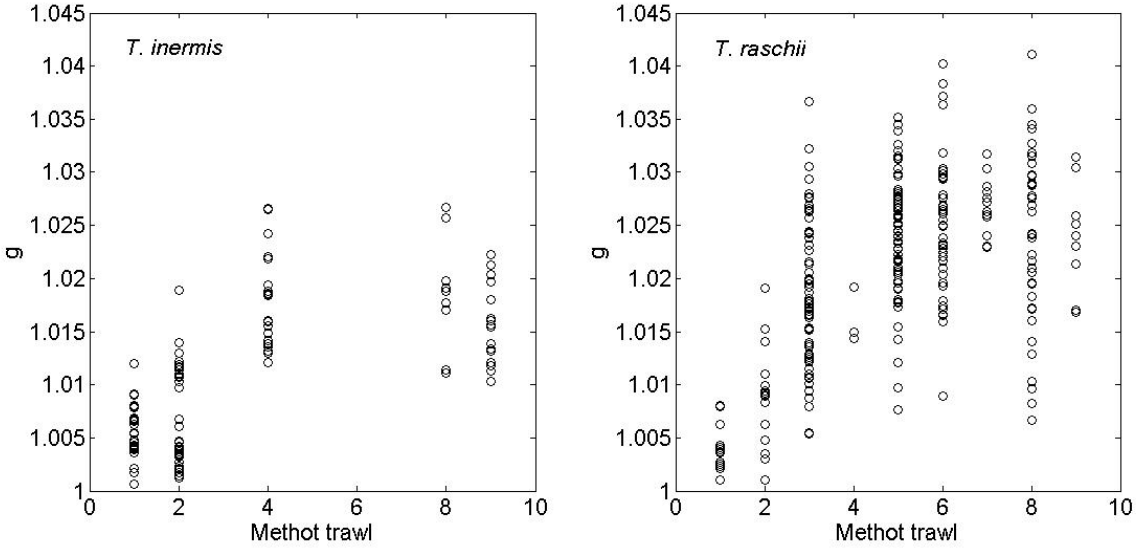

Fig.8. Density contrast for *T. inermis* and *T. raschii* for each MT. Overall *g* values are lower for the East region (MT01,02,03,04) compared to the West (MT05,06,07,08,09).

There was no strong relationship between euphausiid length and *g* for any species or for all species combined, as there was a large variability in *g* between different animals of the same length (Fig. 9). Linear regressions between animal length and *g* indicated a very weak negative relationship for all euphausiids ($R^2 = 0.062$) and for each species individually (*T. inermis* - $R^2 = 0.014$; *T. raschii* - $R^2 = 0.004$; *T. spinifera* - $R^2 = 0.063$).

The temperature surrounding the animals during their measurements was the product of both the ambient temperature the animals were collected from as well as experimental manipulation. To evaluate the complexity of multiple factors impacting *g*, two-way factorial ANOVAs were used to determine the relationship between location, temperature, and the interaction between the two variables on animal density, water density, and *g*. These statistical analyses were performed on each species separately. *T. inermis* were exposed to water temperatures ranging from 0.5°C to 6.3°C and *T. raschii* were exposed to similar temperature ranges of 0.5°C to 6.4°C. Results for *T. inermis* indicated that location, temperature, and the interaction between the two variables had a significant effect on the animal density, the water density, and *g* ($p < 0.001$ for all tests): animal density, water density, and *g* increased at stations located further to the west and

with colder ambient water temperatures, and ambient water temperature was related to station location.

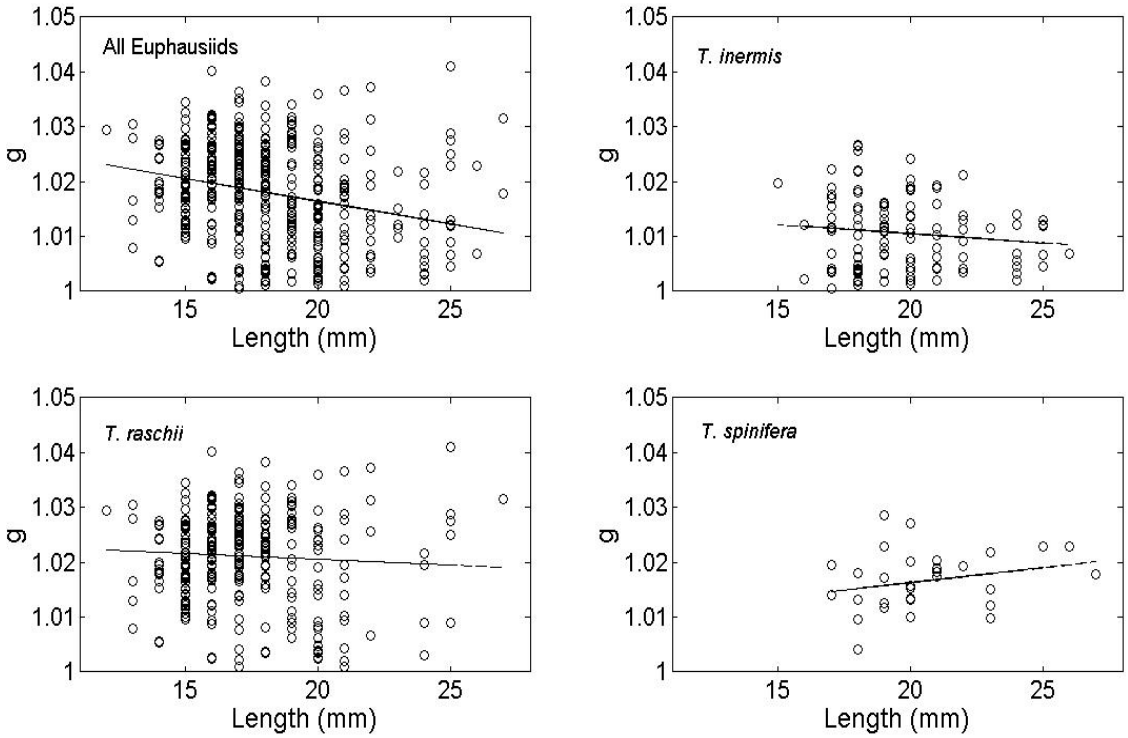

Fig.9. Density contrast (*g*) as a function of animal length for a.) all euphausiids (n=448), b.) *T. inermis* (n=114), c.) *T. raschii* (n = 282), and d.) *T. spinifera* (n = 32). There is a large range in *g* values for all animal lengths. Linear regressions (straight lines in subpanels) showed that there is little correlation between the two variables for all euphausiids and each species. All species: R^2=0.062; g = -0.000825* Length(mm)+1.03; *T. inermis*: R^2=0.014; g = -0.000336* Length(mm)+1.02; *T. raschii*: R^2=0.0035; g = -0.000203* Length(mm)+1.02, and *T. spinifera*: R^2=0.063; g = -0.000545* Length(mm) +1.01.

The relationship between location and water density on *g* was analyzed through two-factorial ANOVAs. This analysis was applied to *T. inermis* and *T. raschii* separately and the results differed for each species. *T. inermis* were exposed to water densities ranging from 1.0252 g ml^{-1} to 1.0282 g ml^{-1}. Results from the two-factorial ANOVA for *T. inermis* indicated that location, water density, and the interaction between the two variables had a significant effect on *g* ($p < 0.001$ for all three results). *T. raschii* were kept

in water with densities with a larger range (1.0234 g ml^{-1} to 1.0282 g ml^{-1}) and yet only location had a significant effect on *g* ($p < 0.001$).

The results from the PCA and previously described two-factorial ANOVAs have indicated that location influences *g*. Furthermore, a piecewise multiple comparison procedure (Dunn's Method) indicated that the western locations (MT05, MT06, MT07, MT08, MT09) were significantly different from the eastern locations (MT01, MT02, MT03, MT04) for both *T. inermis* and *T. raschii* ($p < 0.05$ for all pairwise comparisons between eastern and western sites). The *g* values of *T. inermis* and *T. raschii* were grouped into eastern and western sites and a Kruskal-Wallis one-way ANOVA on ranks was evaluated between the two groups for both species. Results from both ANOVAs indicated that there was a significant difference in *g* between the eastern and western sites ($p < 0.001$, for both species) with the animals from western sites having a significantly lower *g* than those from the eastern sites (Fig. 10).

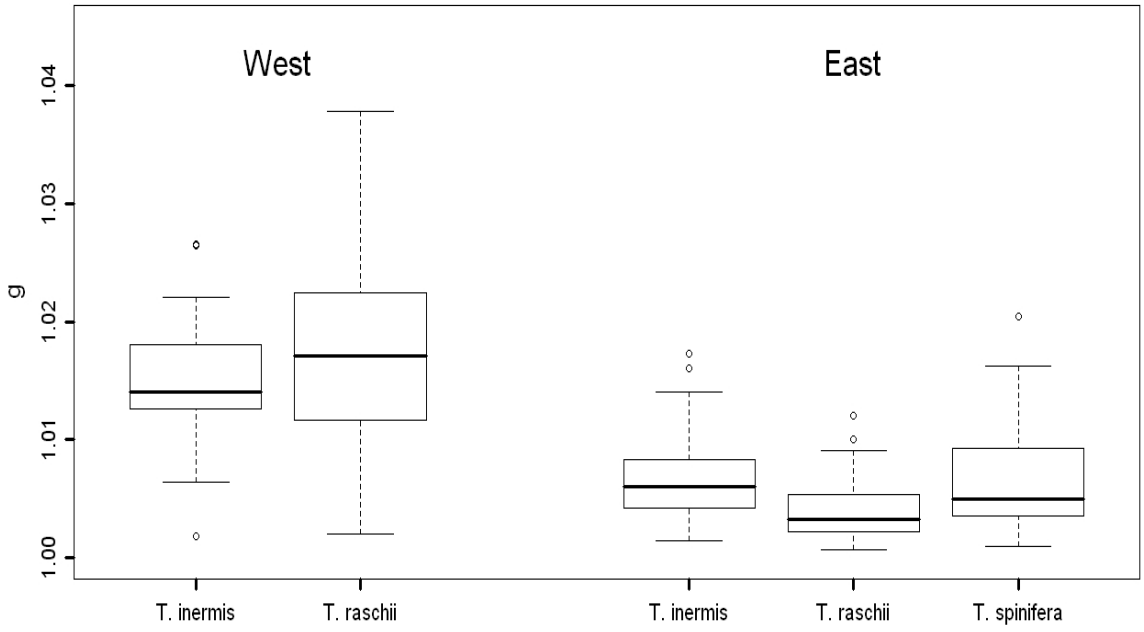

Fig.10. Density contrast (*g*) distributions for different euphausiid species between the East (MT01, MT02, MT03, MT04) and West (MT05, MT06, MT07, MT08, MT09) locations. Density contrast was significantly different between the western and eastern sample sites for euphausiids ($p < 0.001$).

Water column properties at each MT station (rather than the properties of the ambient water in which the animals were kept) indicate that the western stations were characterized by generally colder and denser water with higher chlorophyll concentrations (Table 2). Since location was shown to have an effect on *g*, we examined the hypothesis that differences in chl-a between the sites explained the differences in *g* with location that were observed. The maximum chl-a concentration varied at each location and occurred at different depths (ranging from 16.9 m to 50.0 m). The results from the Pearson correlation between *g* and the chl-a measured at the same depth at which the zooplankton were collected indicated that there was a weak relationship between the two variables ($r^2 = 0.025$, $p < 0.05$). Euphausiids migrate vertically and move throughout the water column over the course of a diel cycle (Schabetsberger *et al*., 2000); thus, a Pearson correlation was also computed between *g* and chl-a integrated over the entire water column which found a significant relationship ($r^2 = 0.172$, $p < 0.001$). The correlation between chl-a and *g* was negative, that is *g* decreased as chl-a increased. Finally, the chl-a data were divided into the same two areas (eastern and western) and t-tests were used to determine whether there was a significant difference in chl-a between the two areas. There was no significant difference between the eastern (MT01,02,04) and western (MT05,07,08,09) locations for the chl-a measured at the depth from which the zooplankton were collected ($p = 0.06$). However, there was a significant difference between the integrated water column chl-a concentration for the eastern and western sites ($p < 0.05$). Chl-a was higher in the eastern MTs compared to the western MTs (Fig. 11).

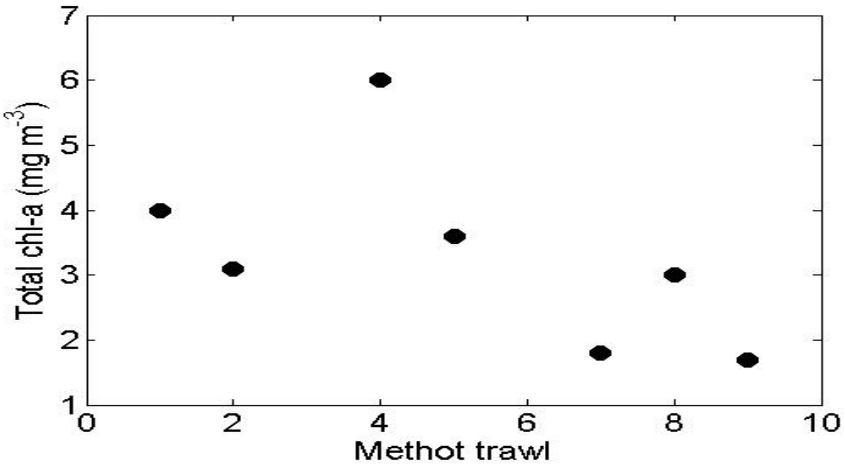

Fig.11. Chlorophyll-a integrated over the water column varied with Methot trawl location. Sites in the western region (MTs 5 and higher) had lower levels of chl-a than eastern sites (MTs 4 and lower).

Furthermore, the mean integrated chl-a of the western sites was 2.45 mg m^{-3} while the mean of the eastern sites was nearly double that at 4.56 mg m^{-3}.

2. Other zooplankton groups

Along with euphausiids, other abundant zooplankton taxa in the Methot trawl catches included copepods and amphipods, however there were relatively few chaetognaths, gastropods, fish larvae, jellyfish, and squid specimens collected. Material properties and length measurements for each zooplankton group were measured, however relatively small data sets did not allow for environmental and spatial analysis to be conducted as was done for the euphausiid data.

a. Copepods. Ninety copepods (*Neocalanus* sp.) were analyzed from MT02 (n = 18), MT04 (n = 31), and MT09 (n = 41). Density contrast ranged from 0.995 to 1.015 with a mean and sd of 1.005 ± 0.006 (Table 3). A linear regression showed little relationship (R^2 = 0.007) between copepod length and *g* . The regression fit was likely affected by the small range in copepod length and by the presence of both positively (g < 1) and negatively (g > 1) buoyant copepods.

b. Amphipods. A total of 66 amphipods (*Themisto libellula*) were collected from MT05 and MT08. Twenty-two amphipods were classified as small (< 20 mm length) and 44 amphipods were classified as large (> 20 mm length). The density contrast of small amphipods ranged from 1.001 to 1.009 with a mean and sd of 1.005 ± 0.002 (Table 3). The density contrast of large amphipods ranged from 1.002 to 1.029 with a mean and sd of 1.013 ± 0.006 (Table 3; Fig. 12).

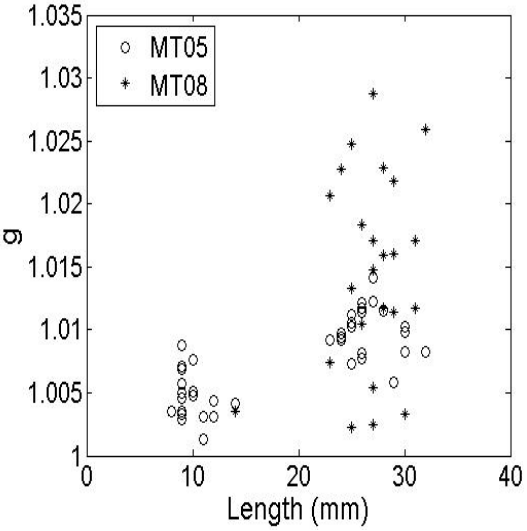

Fig.12. Amphipod density contrast (g) was weakly correlated with animal length. Amphipods from Methot trawl 05 were split between small (<20 mm) and large (> 20 mm) animals, whereas animals from Methot trawl 08 were almost all large animals. The large animals showed a greater range in g values. Density contrast was significantly different between the small and large amphipods (t-test, $p<0.001$). Results from a linear regression showed that R2=0.33 and g = 4.35x10-4*Length (mm) + 1.

A linear regression showed that a weak correlation ($R^2 = 0.33$) existed between amphipod length and *g*. Density contrast varied both between and within the small and large amphipods. The large amphipods had a greater range in *g* than the smaller animals and *g* was significantly different between the two groups (t-test, $p < 0.001$).

c. Chaetognaths. Although they were found in small numbers in multiple MTs, a total of 14 chaetognaths (*Sagitta* sp.) all from MT09 were measured. Their density contrast (*g*) values ranged from 1.007 to 1.026 with a mean and sd of 1.014 ± 0.007 (Table 3). Chaetognaths had the best correlation of all taxa between length and *g* ($g = -7.16 \times 10^{-3} *$ Length(mm) + 1.03; $R^2 = 0.503$).

d. Gastropods. Seventeen gastropods (*Clione limacina*) collected from two MTs (13 from MT06, 4 from MT07) had a *g* ranging from 1.008 to 1.031 with a mean and sd of 1.016 ± 0.006. A linear regression between length and *g* produced a low coefficient of determination ($R^2 = 0.03$).

e. Fish Larvae. Fifteen larval fish (*Theragra chalcogramma*) were collected and measured (6 from MT06, 9 from MT07). Their *g* values ranged from 1.008 to 1.039 with a mean and sd of 1.023 ± 0.008 (Table 3). A linear regression between length and *g* produced a low coefficient of determination ($R^2 = 0.00062$).

f. Jellyfish. Two species of jellyfish were measured, *Chrysaora melanaster* and an unidentified hydromedusa. *Chrysaora melanaster* were too large in size (bell diameters ranged from 15 to 24 cm) for density measurements with the available equipment, so the bells were cut into smaller pieces (n = 36) and measurements performed immediately after this. The mean length, width, and thickness of the pieces were 49 mm, 25 mm, and 8 mm respectively. The density contrast ranged from 1.001 to 1.006 with a mean and sd of 1.003 ± 0.001 (Table 3). The density contrast was calculated for the entire body of the unidentified jellyfish species (n=4), and ranged from 1.004 to 1.005 with a mean and sd of 1.005 ± 0.001 (Table 3).

g. Squid. The density of the squid mantle was measured in a laboratory using the pipette method, while the densities of the squid beaks were measured in the laboratory using the titration method, but with glycerine as the titrate instead of a hypersaline solution. As noted previously, measurements on the squid pens were not possible due to deterioration

of the samples. Seven pieces of squid mantle were measured and *g* ranged from 1.023 to 1.116 with a mean ± sd of 1.073 ± 0.030 (Table 3). The mantle pieces were slightly deteriorated, so *g* may differ from that of live tissue. Fifteen squid beaks were collected and separated into upper and lower jaw pieces for a total of 30 density measurements. Their *g* ranged in value from 1.125 to 1.180 with a mean of 1.149 ± 0.013 (Table 3). The squid beaks showed no evidence of deterioration.

C. Sound speed

Sound speed contrast data were collected for those zooplankton taxa abundant enough to fill a 26 ml or 84 ml PVC T-tube measurement chamber. The sound speed contrast was measured for groups of animals from the same taxon in each haul. When a particular taxon was abundant within the MT, several different groups of those animals were measured for their *h* value. In total, *h* was measured for 11 separate groups of euphausiids representing all MTs except MT06. The number of group measurements of *h* for each taxon were: copepods (3), amphipods (3), gastropods (1), jellyfish (*Chrysaora melanaster*, 8), and squid mantle (2). Three trials were conducted for each group and the results were averaged. The mean percent difference in *h* between trials was 0.076%. As a taxon, euphausiids had both the greatest number and the widest range of *h* measurements (range 0.990 to 1.017; mean 1.006, sd 0.008; Table 3). The two squid mantle measurements were the most consistent with $h = 1.010$. Copepods, amphipods, and jellyfish also displayed a range in *h* values (Table 3). Location was found to be an important factor influencing *g*, hence euphausiids (the taxon with the most measurements of *h*) were separated into eastern (MT01, MT02, MT03, MT04) and western (MT05, MT07, MT08, MT09) groups and a t-test was used to evaluate the difference in *h* between the two groups. Unlike the density data, there was no significant difference in *h* of groups of euphausiids from the eastern (n = 4) and western (n = 7) sites, although this result may have been affected by the small sample size for the sound-speed measurements.

IV. DISCUSSION

Although there are a small number of previous studies on the material properties of several of the taxa we measured, there have been no such measurements on specimens from the Bering Sea. There are also several relatively common zooplankton groups (such as chaetognaths) which have had no information reported about their material properties at all prior to this study. A major contribution of this study are measurements of zooplankton material properties from this ecosystem; these data (Table 1) can be used in scattering models to provide more accurate estimates of zooplankton biomass or abundance.

Little is known about how material properties might be affected by or related to factors such as animal length, geographic location, surrounding environmental conditions, age, gender, fecundity, feeding state, or numerous other factors which are likely to affect the body composition of these organisms and thus their density and sound speed (Chu *et al.,* 2000; Chu and Wiebe*,* 2005; Forman and Warren, 2009). Therefore, we also examined the effects of various parameters on the material property measurements*,* focusing principally upon euphausiid *g,* the zooplankton group and material property for which we had the most observations. The variables considered were species, length, water temperature, water density, location, and water column chl-a concentration as a proxy of zooplankton prey abundance. Principal component analysis determined how these different explanatory variables were related to one another. Separate analyses were used to further examine specific relations between a given variable (or variables) and *g*.

A. Density contrast

All of the explanatory variables we examined appeared to contribute to the variance in *g* to some degree, but the location from which the animals were collected had the strongest relationship with *g*. Both euphausiid density and *g* were greater at western MT locations than at eastern stations, and increased with increasing water density and salinity, and decreasing temperatures. These relationships occurred for both ambient (at the MT station) or experimental (in the tank the animals were maintained) conditions. However, if all other factors are constant and the animals are not altering their own

density, increasing ambient water density should cause a decrease, not an increase, in *g*. We suspect that the increase in *g* was due to an increase in animal density at the western stations (Fig. 6) which was greater than any increase in ambient water density; as *g* was significantly different between the western and eastern sample sites for euphausiids ($p < 0.001$). These western sample sites were characterized by colder water and higher chlorophyll concentrations.

Water temperature changes both spatially and seasonally and can alter the material properties of zooplankton throughout the year (Forman and Warren, 2009). Changes in lipid composition were suggested by Køgeler *et al.* (1987) to explain the differences in *g* between seasons. Many zooplankton increase their lipid composition in colder months as a means to store energy through winter (Campbell and Dower, 2003). Female euphausiids alter their lipid composition throughout egg reproduction (Smith, 1991). Such changes in lipid composition are likely triggered by temperature changes, though the exposure time to different temperatures in our experiments (several hours to a day) may have been too short to allow the animals to adjust their body composition. Long term exposure to the ocean temperatures at the locations from which the euphausiids were collected (average water column temperature for the stations in the eastern group was 2.6 ºC compared to 0.4 ºC for the west) could partially explain the difference in animal density between MTs (Fig. 6).

It is also possible that zooplankton that are well-fed have different material properties than those animals without a sufficient food supply. The concentration of phytoplankton varies both spatially and seasonally, and we used chl-a concentration as a crude indicator of the abundance of phytoplankton, the primary prey for euphausiids in these waters. Chl-a had a significant correlation with animal density and *g* ($r^2 = 0.17$), with western MT sites having less chlorophyll than eastern sites. The r^2 value is fairly low, but the mean chl-a values differ by a factor of two (western region = 2.45 mg m^{-3}; eastern region = 4.56 mg m^{-3}). This difference may be substantial when considering the difference in surface chl-a values between a spring bloom (3.5 – 6.0 mg m^{-3}) and summer months (0.8 – 1.0 mg m^{-3}) where nutrient consumption limits phytoplankton production for the middle and outer shelf of the Bering Sea (Iida and Saitoh, 2007). The difference

in mean chl-a concentrations between the eastern and western sites is not as large as the difference between a spring bloom and and the subsequent decline for a similar region. However, the difference might be great enough to potentially influence the material properties of euphausiids. We did not examine the specific mechanism responsible for this relationship; it may be the result of the phytoplankton prey being less dense than the euphausiids and as the euphausiids eat the less dense material they themselves become less dense, or it may be that well-fed animals are storing energy as lipids which will affect their density relative to the surrounding seawater. Information on euphausiid gut contents, gut volume, and phytoplankton densities would need to be measured to determine the differences in *g* for euphausiids that are well- and poorly-fed. Future studies examining material properties of zooplankton should include an examination of lipid content in order to better resolve this issue.

We found differences in *g* for the same species due to changing environmental conditions over relatively small distances (10s – 100s km); differences due to environmental conditions that vary with location may explain the differences between our data for *T. inermis* and *T. raschii* from the Bering Sea and those of Køgeler *et al.* (1987) for the same species of euphausiids collected off Norway. Greenlaw and Johnson (1982) also measured the density contrast of *T. raschii* in two widely separated locations; the density contrast of *T. raschii* from Norway ranged from 1.013 to 1.018 while *g* ranged from 1.045 to 1.050 in Saanich Inlet, British Columbia. Results reported by Greenlaw and Johnson (1982) for *T. raschii* in Norway are similar to our *g* estimates for the same species in the Bering Sea, while their results for *g* of *T. raschii* from British Columbia are similar to Køgeler *et al.* (1987)'s results from the Barents Sea. Variation of material properties among different locations, environmental conditions, and times of year is not yet well understood.

Even though the euphausiid species we examined are of the same genus and have a roughly similar morphology, there were enough differences between each species to suggest an effect on *g,* though we were not able to conclusively separate a species effect from that of sample location. Køgeler *et al.* (1987), working in the Barents Sea, examined the material properties of three euphausiid species (*Thysanoessa inermis*, *T.*

raschii, and *Meganyctiphanes norvegica*) over the course of a year. The *Thysanoessa* species they measured are also the dominant euphausiids on the Bering Sea shelf (Smith, 1991). Although Køgeler *et al.* (1987) did not test for any significant difference in density contrast values among the three euphausiid species, they showed that *g* values were slightly different among the species, and that *g* fluctuated with season. The density contrast of *T. inermis* and *T. raschii* fluctuated in a similar pattern in which the maximum *g* occurred in February and the minimum *g* occurred in mid-November for *T. inermis* and mid-December for *T. raschii.*

The *g* values that we report are generally smaller and have a wider range, and yet they overlap with the range of measurements described in Køgeler *et al.* (1987) for the same euphausiid species (this study: 1.001 to 1.041; Køgeler *et al.* (1987): 1.022 to 1.054). Greenlaw and Johnson (1982) report *g* values for *T. raschii* that range from 1.045 to 1.050 for animals collected in the summer from Saanich Inlet, British Columbia, to 1.013 to 1.018 for animals collected off Norway in the winter. A comparison with *g* values for other euphausiid species is also appropriate, as in the absence of better information, the material properties of a particular taxon has often been applied to modeling the scattering of other taxa. The *g* values we obtained for *Thysanoessa* spp. appear to be somewhat lower than *g* values obtained for *Euphausia superba*, for which several material property studies exist. Greenlaw and Johnson (1987) reported that *g* ranged from 1.021 to 1.040 for *E. superba*. Chu and Wiebe (2005) gave a range in *g* for *E. superba* from 1.017 to 1.036. Data on *E. superba* from these studies (as well as Foote, 1990) are often used for scattering models for any euphausiid-like animal, even though there are large differences between different euphausiid species particularly in their size (adult *E. superba* are roughly two to three times as large as *T. inermis* or *T. raschii*).

The density contrast of our copepods ranged from 0.995 to 1.015 with a mean of 1.005 ± 0.006. The mean copepod *g* value from our results lies within the range of copepod density measured by Køgeler *et al*. (1987). However, it is important to note that the copepod species examined in our study (*Neocalanus* sp.) are larger (7 to 9 mm in length) compared to the copepods examined in Køgeler *et al*. (1987) (*Calanus*

finmarchicus, 2.2 to 3.0 mm and *Calanus hyperboreus*, 3.5 to 5.5 mm in length). The density contrast of copepods measured by Køgeler *et al.* (1987) ranged from 0.999 (February through September) to 1.003 in late-February for *Calanus hyperboreus*; for *Calanus finmarchicus*, *g* ranged from 0.996 at the end of July to 1.010 in late-February. Unlike the measurements of euphausiids, both our study and that of Køgeler *et al*. (1987) measured copepods with positive and negative buoyancy ($g < 1$): approximately a quarter of our copepods were less dense than the seawater, while Køgeler *et al.* (1987) showed that copepods were less dense than seawater the majority of the year and only became denser immediately prior to spawning in March. Copepods with both positive and negative buoyancy have also been reported elsewhere for the same genera and species. *Calanus* sp. found in Antarctic waters were all measured to have densities less than seawater (Chu and Wiebe, 2005), but none of the copepods measured by Greenlaw and Johnson (1982), including representatives of the species *Calanus finmarchicus,* were less dense than seawater. It is possible that the majority of the copepods measured in this study had recently spawned or otherwise did not contain sufficient lipid stores to be less dense than water.

Our examination of the effect of animal length on *g* revealed that for most zooplankton taxa in this study there was little or no correlation between the two variables. Amphipods ($R^2 = 0.33$) and chaetognaths ($R^2 = 0.50$) were the only taxon with a coefficient of determination greater than 0.10 between length and *g*. Though our results indicated no significant relationship between euphausiid length and *g*, we calculated a linear regression between animal length and *g* for euphausiids in order to compare to the linear regressions for the same species found in Køgeler *et al.* (1987). Their euphausiids (*T. inermis* and *T. raschii*) ranged in length from 10 to 25 mm while our euphausiids ranged in length from 12 to 27 mm. They provided multiple regression equations ($g = a*\text{Length(mm)} + b$) for each month that data were collected. The slopes for their linear regressions were all small negative numbers (ranging from $-0.01\text{x}10^{-3}$ to $-2.5\text{x}10^{-3}$ with a mean slope of $-1.27\text{x}10^{-3}$) and their coefficients of determination ranged from $R^2 = 0.01$ to $R^2 = 0.90$. We calculated a similar slope of $-0.93\text{x}10^{-3}$ for the linear regression between euphausiid length and *g* and a small coefficient of determination ($R^2 = 0.06$). Greenlaw

and Johnson (1982) examined euphausiids of the genus *Thysanoessa* (but from unspecified locations) and demonstrated a positive relationship between animal length and the density contrast, but their data represented a very small range (15 to 18 mm) of lengths. Chu and Wiebe (2005) also reported a positive correlation between euphausiid length and *g*, however all of their animals were larger (25 - 52 mm) and of a different species (*Euphausia superba*) than the euphausiids in our study.

B. Sound speed contrast

While density contrast was measured for individual zooplankton, *h* was measured on groups of animals (Table 3). Unfortunately the sound speed contrast could not be measured for all zooplankton groups since not enough individuals of some taxa were collected. Overall, *h* was fairly close to unity for all zooplankton groups for which measurements were made and in some cases it was less than one, which signifies that sound travels slower through the group of zooplankton compared to the surrounding seawater. It is likely that these bulk measurements, containing multiple sizes and species for each taxon, are intrinsically more variable than measurements made on individuals of a single type and size. The sound speed contrast for euphausiids ranged from 0.990 to 1.017 with a mean and standard deviation of 1.006 ± 0.008, lower than *h* measured for two of the same species (a mixture of *T. inermis* and *T. raschii*) by Køgeler *et al*. (1987), who reported a mean of 1.026 ± 0.005. Greenlaw and Johnson (1982) measured *h* for *T. raschii* ranging from 1.032 to 1.045, which is also higher than the *h* measurements collected for euphausiids from the Bering Sea. Similarly, Bering Sea euphausiid *h* measurements were lower than the average *h* value measured for *E. superba* by Chu and Wiebe (2005) which was 1.030 ± 0.004 and by Foote (1990) which was 1.0279 ± 0.0024. Euphausiid *h* did not exhibit the east-west spatial pattern observed for euphausiid *g*. Bering Sea copepod *h* measurements were lower then the results Køgeler *et al*. (1987) reported for a different genus, species, and animal size of copepod: our average *h* for *Neocalanus* sp. copepods was 1.007 ± 0.004, while Køgeler *et al*. (1987) for several species of the genus Calanus showed a mean *h* of 1.027 ± 0.007. Greenlaw and Johnson (1982) report similar *h* values to this study ranging from 1.006 to 1.012, even though they measured a smaller copepod species (*Calanus plumchrus*).

Uncertainty in *h* is partly due to interstitial water between the animals being measured when using displacement volume to estimate volume fraction (Eq. 6), which may explain some of the variation in *h* for each zooplankton taxon. It is preferable that animals be uniformly distributed within and appear to fill the horizontal section of the measurement tube (Foote, 1990). Køgeler *et al*. (1987) reported that the maximum volume fraction within their measurement chamber was 65%, but the mean volume fraction in this study ranged from 63% to 100% with a mean of 89%. Indirect methods of measuring volume fraction involve measuring the resistivity of a group of animals and then calculating its theoretical volume fraction; Chu *et al.* (2000) showed that this method can significantly reduce the error in calculating *h*, but this technique has not yet been widely used.

C. Effect on predictions of target strength (TS)

Material properties appear to be a function of the environment as well as a function of the physical parameters of the various zooplankton groups. It is very difficult to understand the relationship of each parameter on *g* considering many of the factors are inter-related (e.g. location, water temperature). The importance of these relationships is that very small differences in *g* and *h* (0.01 or less for each) that may result from differences in, for example, location, species, or animal size can produce different TS values that will result in vastly different estimates of numerical abundances of animals when used in conjunction with acoustic backscatter survey data. Forman and Warren (2009) showed that using the lowest, average, and highest values of *g* and *h* that they measured for coastal zooplankton can result in differences in population estimates of up to three orders of magnitude. Given the wide range of *g* and *h* values in the literature and the fact that bioacousticians often use material property values from species other than the ones they are studying (primarily because the data they need do not exist), it is imperative that more material property measurements are made. For example, many studies use the values reported for *Euphausia superba* by Foote *et al.* (1990) or more recently Chu and Wiebe (2005) for any fluid-like crustacean, even when the animal being studied is either much smaller in size or a completely different family or order of animal.

Chu and Ye (1999) show that the differential backscattering cross section (σ_{bs}) is

proportional to the square of the sum of the deviations of *g* and *h* from unity ($\sigma_{bs} \alpha (\Delta h + \Delta g)^2$ where $\Delta h = h-1$ and $\Delta g = g-1$). Since σ_{bs} is related to target strength by the equation $TS = 10\log\sigma_{bs}$ (Stanton *et al.*, 1996), we can calculate how much TS will change when different *g* and *h* values are used. Both *g* and *h* are proportional to the backscattering cross-section; however, we cannot be certain that *g* and *h* are correlated given that *h* can only be measured on groups of animals while *g* is measured for individual animals. For instance, euphausiids measured in this study had a range in *g* from 1.001 to 1.041 and a range in *h* from 0.990 to 1.017, which would result in TS estimates that vary by as much as 16 dB. As a difference in TS of 10 dB corresponds to an order of magnitude difference in the numerical density of a scatterer, the variation in *g* and *h* from our study needs to be taken into account to produce zooplankton population estimates that are accurate enough for studies of ecosystem processes.

Since location appeared to be a significant factor influencing *g* for euphausiids in the Bering Sea, the variation in TS was calculated using the ranges in *g* and *h* found in the eastern and western groups. TS estimates could vary by 19.5 dB for eastern euphausiids and 16.7 dB for western euphausiids. These large dB ranges are the maximum differences that could occur within a population based on data collected in the Bering Sea; the likely range of TS estimates based on the combinations of mean *g* and *h* observed in our data from each MT may be substantially smaller. In addition to estimating the maximum possible difference in TS due to *g* and *h* measurements of euphausiids in the Bering Sea, a more likely estimate of the variability in TS can be found by computing the proportional effect on the backscattering cross-section (σ_{bs}) from the average *g* and *h* for each MT (using the equation presented in Chu and Ye, 1999). Using this method, the estimated difference in the range of TS values (between 95% confidence bounds approximated as twice the standard error of the mean) was 5.7 dB for all euphausiids, 9.0 dB for the East, and 4.8 dB for the West. The larger range for the East region is the result of g values being very close to unity, where small changes in *g* will produce larger variations in TS. The actual TS distribution for a population of animals may need to be calculated on an individual-by-individual basis to determine the impact of the variability in material properties on numerical estimates of animal abundance.

D. Conclusions

This study presents material property values for Bering Sea zooplankton. We measured the material properties for euphausiids, copepods, amphipods, chaetognaths, gastropods, fish larvae, jellyfish, and body parts of squid. In those cases where there were prior measurements of the same taxa using specimens collected from different regions, our measurements showed significant variation; these differences suggest that uncertainty in scattering model predictions should be reduced if material property values are specific to each target taxon in the location being studied. Potentially, if an environment is relatively stable from year to year, the material properties of a particular zooplankton group may also be stable. The only way to verify this is to measure the material properties for a specific location and group of animals during the time period of interest. If material properties are shown to be stable or predictable, then less frequent measurements of material properties would be needed. With improved knowledge of material properties, including what factors cause these properties to change, as well as other scattering model inputs such as animal orientation (Demer and Conti, 2005; Warren *et al.* 2002); more accurate estimates of zooplankton abundance and distribution could be made from acoustic surveys which would improve our ability to understand the status and trends of these populations.

CHAPTER 2

Use of a distorted wave Born approximation (DWBA) model to estimate the target strength (TS) of Bering Sea krill

I. Introduction

Euphausiids are an important part of the Bering Sea ecosystem. These crustacean zooplankton are prey for many species, including murres (Decker and Hunt, 1996), northern fur seals (Sinclair, 1994), puffins (Hatch and Sanger, 1992), and most notably walleye pollock (*Theragra chalcogramma*) (Bailey, 1989; Lang *et al.*, 2000, 2005) which are the target of one of the largest single-species fisheries in the world (FAO 2009). There is interest in a quantitative estimate of the abundance of euphausiids in the eastern Bering Sea because of the trophic linkage between euphausiids and pollock (Ianelli *et al.*, 2009). Acoustic-trawl resource assessment surveys conducted in the Bering Sea by the National Marine Fisheries Service (Honkalehto *et al.*, 2009) provide a potential source of this information. Acoustic surveys allow sampling of large areas at high spatial and temporal resolution (Simmonds and MacLennan, 2005), but net sampling must still be conducted to ground-truth the acoustic data and determine the types of animals being detected (Kasatkina *et al.,* 2004). Once the identity of the dominant acoustic targets are known, a model of the acoustic scattering from these targets is required to convert acoustic backscatter measurements into units of animal abundance and biomass (Foote and Stanton, 2000).

The prevailing approach to modeling the scattering of euphausiids is via physics-based scattering models, which require input parameters describing the acoustic wave (frequency or wavelength) and the target (its shape, length, orientation relative to the acoustic wave, and material properties; Stanton and Chu 2000; Lavery *et al.* 2002; Demer and Conti, 2003; Lawson *et al.* 2006). The material properties used in acoustic modeling are: density contrast (g), the ratio of the density of the animal and the density of the ambient seawater, and the sound speed contrast (h), the ratio of the speed of sound of the animal and the surrounding seawater. Material property data are often measured through

laboratory studies of individual specimens (Greenlaw and Johnson, 1982; Køgeler *et al*., 1987; Forman and Warren, 2010), although these measurements have also been made at sea (Chu and Wiebe, 2005; Smith *et al.,* in press).

A variety of scattering model formulations have been proposed for euphausiids. Initially, euphausiids were modeled as straight cylinders (Stanton 1988a, b), but more advanced models considered their shape to be deformed (bent) cylinders (Stanton *et al.* 1993a; Stanton *et al.*, 1993b; Stanton and Chu, 2000). Ray-based solutions were used to compute the scattering at different euphausiid orientations; however, ray-based models work best for angles of incidence near normal to the lengthwise axis of the body (Stanton *et al.* 1993b) and are only valid at high frequencies (Urick, 1983).

More recently, the distorted wave Born approximation (DWBA) model has been used to model the backscatter from euphausiids. The DWBA model is valid for all acoustic frequencies, can be evaluated for all angles of orientation (Chu *et al.*, 1993), and can be applied to arbitrary shapes (Stanton *et al.,* 1998). In the DWBA model, a scattering function is integrated over the length of the axis of the body, taking into account the phase shift that results from the bent body. The model assumes that the targets are comprised of weakly scattering material, which is true for euphausiids. The general formula for modeling acoustic scattering with the DWBA model was first given by Morse and Ingard (1968) as:

$$f_{bs} = \frac{k^2}{4\pi} \int\int\int (\gamma_\kappa - \gamma_\rho) e^{i2k_2 r_{pos}} dv \quad . \tag{9}$$

The integration is within the volume (v) of the body and has a position vector (r_{pos}), k_2 is the incident wave number vector inside the body, and γ_κ and γ_ρ are terms used to describe the material properties within the body. The parameters γ_κ and γ_ρ are expressed in regards to the compressibility (κ), density contrast (*g*), and sound speed contrast (*h*) and are described as follows:

$$\gamma_\kappa \equiv \frac{\kappa_2 - \kappa_1}{\kappa_1} = \frac{1 - gh^2}{gh^2} \tag{10}$$

$$\gamma_\rho \equiv \frac{\rho_2 - \rho_1}{\rho_2} = \frac{g - 1}{g} \tag{11}$$

where $$\kappa = (\rho c^2)^{-1}; h = \frac{c_2}{c_1}; g = \frac{\rho_2}{\rho_1} \quad . \qquad (12)$$

Since the general formula for the DWBA model is complex and requires knowledge of the animal's shape and material properties in three dimensions, a simplified form of the DWBA model with only one integral has been developed (Stanton *et al.*, 1993a). The single integration assumes that the cross-section of the elongated zooplankton is circular throughout the length of the body and the material properties are constant throughout the animal; therefore the integration follows the length of the body (Stanton *et al.*, 1993a; Stanton *et al.*, 1998; Stanton and Chu, 2000). It is written as follows:

$$f_{bs} = \frac{k}{4} \int_{r_{pos}} a(\gamma_\kappa - \gamma_\rho) e^{2ik r_{pos}} J_1 \frac{(2 k_2 a \cos \beta_{tilt})}{\cos \beta_{tilt}} |dr_{pos}| \qquad (13)$$

where a is the radius of the euphausiid as it changes along the length of the animal's body (L), $ß_{tilt}$ is the angle between the incident wave ($\mathbf{k}_i$) and the cross section of the cylinder at each point along its axis, and J_1 is the Bessel function of the first kind of order one. The scattering amplitude, $f_{bs,}$ is related to the backscattering cross section of the target (σ_{bs}) and target strength (TS) by the following relation (Urick, 1983; Medwin and Clay, 1998):

$$TS = 10 \log_{10} |f_{bs}|^2 = 10 \log_{10} \sigma_{bs} \qquad (14)$$

TS is a logarithmic measure of the proportion of the incident energy backscattered from the target measured in units of dB relative to 1 m^2.

TS predictions from the DWBA model have been experimentally validated for krill near broadside incidence with angles less than 15-30º; however, the model predictions of TS at larger angles in the same experiment were approximately 5-10 dB lower than direct measurements (McGehee *et al.,* 1998). For modeling purposes, each euphausiid is divided into multiple cross-sectional areas and the energy reflected by each section is calculated separately and added together for the entire animal. At broadside incidence the cross-sectional area of the animal reflecting acoustic energy is larger than for end-on scattering which results in a higher TS.

The DWBA model may not properly capture the phases of the backscattered signal for angles away from normal incidence. Demer and Conti (2003a) proposed that the variability in the phases had three possible explanations: scattering variability in a field with stochastic noise, krill shape is more complex than the assumed cylinder with varying radii, and krill flex their body as they swim. They attempted to account for this phase variability using a stochastic distorted wave Born approximation (SDWBA) model validated for Antarctic krill (Demer and Conti 2003a, 2003b). Unfortunately their potential explanations for phase variability in echoes from euphausiids have not been conclusively demonstrated or individually analyzed and there is yet no consensus on the best model for euphausiid scattering.

The DWBA model has been more widely used than the SDWBA to model backscatter of euphausiids (Lawson *et al.*, 2006; Amakasu and Furusawa, 2006; Lee *et al.,* 2008; Lawson *et al.*, 2008) as well as other animals such as mackerel (Gorska *et al.*, 2005), Japanese anchovy (Miyashita, 2003), salps (Wiebe *et al.*, 2009), and squid (Jones *et al.*, 2009). Recent studies suggest that euphausiids spend most of their time at orientations where they are nearly horizontal in the water column degrees of horizontal (Demer and Conti, 2005, Conti and Demer, 2006; Lawson *et al.*, 2006), and for this range of animal orientations there may be little difference between DWBA and SDWBA model predictions. For these reasons we elected to use the DWBA model parameterized using recent measurements of the material properties and shape of Bering Sea euphausiids (Smith *et al.*, in press) to estimate TS, and evaluate the effects of animal shape, length, material properties, orientation, and curvature on these estimates. Results from the DWBA and SDWBA models were compared to determine any differences in TS between the two models when applied to Bering Sea euphausiids.

II. Methods

Animal length, shape, species, and material properties were measured at sea for live euphausiids (Smith *et al.*, in press) collected in short tows made near the surface at night using a Methot trawl (MT; Methot, 1986). Zooplankton samples were collected at nine stations from 20 June to 09 July, 2008 during the Bering Sea acoustic-trawl pollock

survey aboard the NOAA Ship *Oscar Dyson*. These data, as well as several different distributions of animal orientation from the literature, were used to parameterize the DWBA model. Since strong species-specific differences in length and material properties were not observed in these data (Smith *et al.*, in press), euphausiids of all species are modeled using the same parameters. The effect of each model parameter on TS estimates for acoustic frequencies from 10 to 1000 kHz was calculated. Methot trawls conducted on euphausiid layers during daytime were used for comparisons of acoustic and net capture estimates of euphausiid density.

A. Model Parameterization and Sensitivity

Target strength predictions from the single integration DWBA model (equations 13 and 14) rely on the shape of the euphausiids (L and *a*), their material properties (γ_κ and γ_ρ), and their orientation and curvature ($ß_{tilt}$).

1. Animal Shape

Chu *et al.* (1993) described the shape of the euphausiids using a taper function:

$$a(z) = a_0 * \sqrt{[1 - (\frac{z}{(L/2)})^T]} \quad (15)$$

where T is the taper variable, a_0 is the radius at the midsection of the euphausiid (z = 0), and L is the length of the animal from the anterior tip of its eye stalk to the posterior tip of its telson (Foote, 1990; McGehee *et al.*, 1998, Demer and Conti, 2005). Previous studies of krill (Chu *et al.* 1993, Lawson *et al.* 2006) used a taper value of 10 (taper occurs rapidly near the edge of both ends of the animal), but a taper variable equal to 2 (taper is gradual and begins near the mid-section of the animal) better described the shape of the Bering Sea euphausiids. However, a more realistic shape model was created by measuring the width, which was later used to calculate the radius, in 0.5 mm increments along the length of the body from digitized images of four Bering Sea euphausiids. The radii measurements were normalized as well as the length of the euphausiid body. The radius was normalized by dividing each radii measurement by the largest radius measurement so that the radius values ranged from 0 to 1. The length of the euphausiid 's body was also normalized (to a value of two) and shifted so that the animal's telson was considered to be point -1, the midpoint was 0, and the end of the eye was 1. The

normalized radius measurements were then averaged for all animals, and two shape functions (a smoothly-varying sixth-degree polynomial and a segmented five-part piecewise) were fit to these measurements. The new shape function was based on measurements of four animals but there was little variation between each animal (average standard deviation in normalized radii was 0.04). The sixth-degree polynomial function, the piecewise function, and the two taper functions (with T = 10 and 2), were separately used to describe the shape of the animal in the DWBA model to estimate the TS of euphausiids.

In order to compare the differences in model predictions of TS for the four shapes, the scattering spectra was calculated for each shape function for two different cases, all shapes with the same mean radii (1.5 mm) and different volumes, and all shapes with the same volume but different radii (different radii (r) of each shape: taper (T=10) r = 1.0 mm; taper (T=2) r = 1.1 mm; polynomial r = 1.6 mm; piecewise r = 0.9 mm). In general, TS models are parameterized using length and width measurements (not using animal volume); however, varying volumes can have an effect on TS as well as the frequency response of the scattering. Thus, both scenarios (same radii and varying volumes, varying radii and constant volumes) were examined.

2. Animal length

TS was estimated with the DWBA model for each euphausiid measured in this study using the measured values in animal length, *g*, and *h*. The largest euphausiid length observed in our study was 27 mm, however, other studies have estimated the TS for much larger specimens from other euphausiid species. For comparison, the TS of a 50 mm animal (e.g., an adult Antarctic krill (*Euphausia superba*)) was also calculated.

3. Material properties

Measurements of material properties of live Bering Sea euphausiids (Smith *et al.*, in press) were used to parameterize the TS model. In that study, the density contrast (*g*) was measured for individual euphausiids, whereas the sound speed contrast (*h*) measurements were made on multiple groups of euphausiids from the same MT. Sound speed contrast measurements were taken for multiple groups of euphausiids from the same Methot trawl (MT) and these measurements were averaged together and the average

h value was assigned to each individual euphausiid in that MT. Since there was no strong difference in *g* for the different Bering Sea euphausiid species (Smith *et al*., in press), species was not used as an independent variable in the TS modeling.

The effects of *g* and *h* on TS model predictions were examined by calculating TS values using the minimum, maximum, and average *g* and *h* values observed in the Bering Sea and *g* and *h* values from other studies (Greenlaw and Johnson, 1982; Køgeler *et al*., 1987; Chu and Wiebe, 2005) for an animal with average length and broadside incidence at a frequency of 120 kHz while the other parameters (orientation, shape, length) were kept constant. The average *g* and *h* combinations for Bering Sea euphausiids was examined by parameterizing the model using minimum, maximum, and average values of the reflection coefficient R, a parameter used in several TS equations (Stanton *et al.*, 1993, Stanton *et al*., 1994) that is dependent upon both *g* and *h* ($R = (gh-1)/(gh+1)$). We also examined if *g* and *h* were correlated.

4. Animal orientation and curvature

Animal orientation (θ) is the angle between the line joining the bent cylinder's ends and the horizontal plane (Lawson *et al.* 2006). The DWBA model can estimate TS at all angles of orientation (Stanton and Chu, 2000). In order to determine the influence of orientation on TS estimates, several different Gaussian distributions describing animal orientation were applied to the DWBA model. The normal distribution of orientations observed for euphausiids measured in an aquarium was found to be $N(\theta,\sigma_\theta)=N(45.3,30.4)$ by Kils, 1981 and $N(\theta,\sigma_\theta)=N(45.6,19.6)$ by Endo, 1993, where θ is the mean angle of orientation and σ_θ is the associated standard deviation. Empirically-estimated distributions of *in situ* krill orientation include N(15,5) (Demer and Conti, 2005) and N(11,4) (Conti and Demer, 2006). *In situ* observations of euphausiid orientation include N(9.7,59.3) and N(0,27.3) (Lawson *et al*., 2006).

Both the animal's orientation and the radius of curvature of the animal (ρ_c) are used to define the parameter $ß_{tilt}$. Assuming the echosounder is pointing down through the water column, an animal is at normal acoustic incidence ($\theta = 0°$), aka broadside incidence, if it is horizontal in the water column. At the midpoint of the euphausiid, $ß_{tilt} = \theta$, however this relationship does not hold true along the length of the euphausiid because

of the curvature of its body. The average radius of curvature was determined for the euphausiids examined in this study (using the geometry described in Stanton *et al.* 1989). Assuming that ρ_c remains constant for all euphausiids, only one value of ρ_c was applied for all animals instead of having a different ρ_c value for each individual euphausiid.

B. Estimates of euphausiid numerical density

When multiple targets are within an echosounder's range-gated insonified volume, their echoes sum to form the backscatter return for that volume of water. The logarithmic measure of combined echo intensity from multiple scatterers in a given volume is the volume backscattering strength ($S_{v,}$ dB re 1 m^{-1}) which can be used to estimate the numerical abundance of scatterers (Simmonds and MacLennan, 2005). A Simrad EK 60 echosounder calibrated via the standard target method (Foote *et al*., 1987) was used to measure S_v at five frequencies (18, 38, 70, 120, 200 kHz). The acoustic transducers were located on a lowered centerboard several meters below the ship's hull and 9.15 m below the sea surface. The linear form of S_v is the backscattering coefficient ($s_{V,}$ m^{-1}):

$$s_v = 10^{(S_v/10)} \quad . \tag{16}$$

The measured s_v values and the backscattering cross-section (σ_{bs}) values calculated from the DWBA model were used to quantify the number of animals (N) present in one m^3 of water using the equation:

$$s_v = \sum_{i=1}^{m} N_i \sigma_{bs_i} \tag{17}$$

where m is the number of different types of scatterers in the volume. It was assumed that euphausiids were the dominant acoustic target (m=1).

Concurrent comparisons of s_v and the density of euphausiids estimated from nighttime live Methot tows used to capture specimens for *g* and *h* measurements were not possible. These nighttime tows collected euphausiids in the upper 10-20 m of the water column where s_v data were not available because of the depth of the vessel-mounted transducers and the necessary blanking distance beneath the transducers to account for pulse transmission and transducer ringing. Instead, nine daytime Methot tows that targeted euphausiid scattering layers located well below the sea surface (identified based

on their frequency response and catch composition; De Robertis *et al.*, in press) were used to compare acoustic and net tow estimates of euphausiid numerical density. Material property data from nighttime MTs were used to calculate the associated reflection coefficient (R) value for each MT as well as the East and West regions (regions described in Smith *et al.*, in press). R estimates are very useful in determining the most common *g* and *h* combinations to be used in TS calculations. There were a total of nine daytime tows (DTs) with DT1-6 constituting the East region and DT7-9 comprising the West region. R values were applied to each DT (based on the region) and the length distribution data gathered from each DT were used to estimate a length-weighted σ_{bs} for each daytime tow using the DWBA model. The mean s_v over the portion of the water column sampled by each daytime Methot trawl was calculated, accounting for the mouth area of the net, the amount of wire out during the net deployment, and the setback between acoustic transducers and the net frame. Observed s_v and σ_{bs} were used to solve equation 18 for N, and this acoustically-estimated quantity was compared with numerical density estimated from the flowmeter-equipped Methot trawl. This procedure was followed for all nine daytime MTs.

For these comparisons, it was assumed that euphausiids were the dominant acoustic target (m=1 in equation 17). Methot tows where scattering from age-1 and older walleye pollock occurred in the trawl path were not used for this comparison, since the Methot trawl will not capture those large nekton. However, since we cannot entirely rule out contributions to measured scattering from other targets that we did not collect in our nets (Warren and Wiebe, 2008), the acoustic estimates of the numerical density of euphausiids presented here will likely be overestimates (Warren *et al*., 2003). In addition, since the animals used for material properties measurements were collected from different tows than those used for comparison of numerical densities estimated acoustically and via net capture, there may be additional uncertainty due to the spatial variation in the material properties of euphausiids (Smith *et al*., in press).

Many studies that estimate euphausiid abundance use backscattering information from low (18, 38, or 70 kHz) and high (120, 200 kHz) frequencies to differentiate or identify backscatter as being from euphausiids (Watkins and Brierley, 1996; CCAMLR

2009), and then use the S_v values at 120 or 200 kHz to estimate krill biomass, abundance, or numerical density (Reiss *et al.*, 2008; Warren and Demer, 2010). This study follows the same approach and uses the mean TS estimates and S_v measured at 120 and 200 kHz to estimate euphausiid numerical density.

C. Comparison to other models

TS estimates were calculated using the DWBA model and SDWBA model in order to compare the differences between both models. TS was calculated for both the DWBA and SDWBA models at 120 kHz for animals lengths ranging from 10 to 30 mm with Conti and Demer's (2006) orientation distribution of N(11,4). The SDWBA was not parameterized for Bering Sea euphausiids so parameters from other studies were applied to both the SDWBA and the DWBA. The euphausiid shape was defined by McGehee *et al.* (1998)'s general shape function but was 40% fatter. Material properties used to calculate TS were described by Foote (1990) as $g = 1.0357$ and $h = 1.0279$.

III. Results

Target strength values for individual euphausiids were calculated for all MTs and scattering model input parameters were varied to determine their effect on krill TS. In order to evaluate the influence of one parameter on TS estimates, other parameters were kept constant. When these values were kept constant, the mean material properties and animal length were used (Table 4). Results in each section are given with respect to frequency.

Table 4. Minimum, maximum, and mean and standard deviation of physical and material properties measured for Bering Sea euphausiids (N = 380).

	min	**max**	**mean**
Length (mm)	12	27	18.2
Width (mm)	1	5	2.5
g	1.001	1.041	1.017
h	0.9898	1.014	1.005

A. Animal shape

From measurements of radius along the length of the body, an average euphausiid

shape was defined by fitting a sixth-degree polynomial to the data:

$$a = 0.83z^6 + 0.36z^5 - 2.1z^4 - 1.2z^3 + 0.63z^2 + 0.82z + 0.64 \quad (18)$$

where z is the normalized length of the animal ranging from -1 to 1 and a is the animal radius in mm. The same data can also be described by the following piecewise function :

$$a = \begin{cases} z = -1 \text{ to } -0.95 & a = 5z + 5 \\ z = -0.95 \text{ to } 0 & a = 0.79z + 1 \\ z = 0 \text{ to } 0.35 & a = 2z + 1 \\ z = 0.35 \text{ to } 0.45 & a = 1.7 \\ z = 0.45 \text{ to } 1 & a = -2z + 2.6 \end{cases} \quad (19)$$

The polynomial shape function is smoothly-varying along the animal length and resembles the actual animal shape more closely. In contrast, the piecewise function has sharp changes in the shape of the animal along the body length. The taper function (using both taper variables T=10 and 2) assumed that the euphausiid was symmetrical while the polynomial and piecewise functions do not (Figure 13).

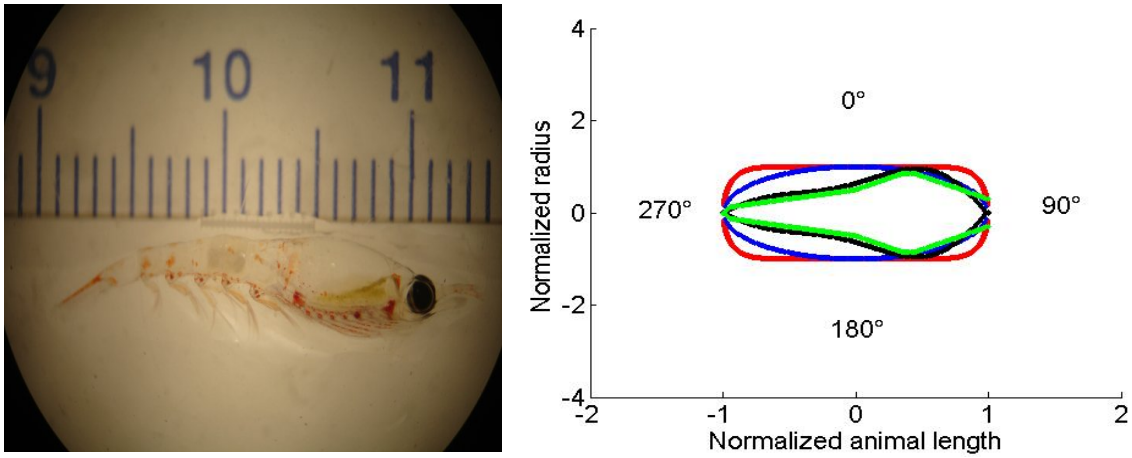

Fig. 13. a.) An image of one euphausiid where the scale is in cm. b) Different functions used to define the euphausiid shape: taper (T=10) (red), taper (T=2) (blue), polynomial (black), and piecewise (green). The incidence angle is also included where 0° is broadside incidence. Notice that the polynomial and piecewise functions more accurately represent the shape of euphausiids.

TS was calculated for all euphausiids from all MTs at 38 kHz, 120 kHz, and 200 kHz and differed depending on which animal shape function was used (Table 5).

Table 5. Mean TS estimates calculated for individual krill using observed lengths, widths, *g*, and *h* values regardless of MT. Calculations were made for three frequencies (38 kKz, 120 kHz, and 200 kHz) using four different euphausiid shape functions and an orientation of broadside incidence.

Shape	**38 kHz**	**120 kHz**	**200 kHz**
Taper (T = 10)	-103.0	-84.7	-79.4
Taper (T = 2)	-105.6	-87.0	-81.1
Polynomial	-110.7	-91.7	-85.0
Piecewise	-113.5	-94.3	-87.1

The polynomial function is the preferred shape function in this study since it gives the best shape description of the euphausiids relative to the other shape functions. Even though the taper function (T = 10) is the most commonly used equation to model euphausiid shape (Chu *et al*., 1993; Lawson *et al.*, 2006), it estimates the TS of an individual euphausiid to be 7 dB higher than the estimate produced from the polynomial function and nearly 10 dB higher than the estimate generated from the piecewise function. Similar TS calculations were made for multiple frequencies (ranging from 10 to 1000 kHz) for an individual animal with the mean length, *g*, and *h* values and a radius of 1 mm (Figure 14a). The volume of each shape with a radius of 1 mm was: taper (T = 10) V = 5.98 mm^3, taper (T = 2) V = 5.03 mm^3, polynomial V = 2.34 mm^3, and piecewise V = 1.68 mm^3. The resulting higher TS values are not unexpected considering the animal volume is larger for both taper functions than for the more realistic polynomial or piecewise shapes. (Figure 13). To compare different shaped animals with an equivalent volume, TS was also calculated as a function of frequency for animals with the same volume of 5.98 mm^3 (Figure 14b). To maintain the same volume, the radius for each shape function was different (taper (T = 10) r = 1 mm; taper (T = 2) r = 1.1 mm; polynomial r = 1.6 mm; piecewise r = 1.89 mm). The polynomial and piecewise functions have smaller TS values compared to the taper function. Use of different shape models also changes the shape of the TS curve as a function of frequency.

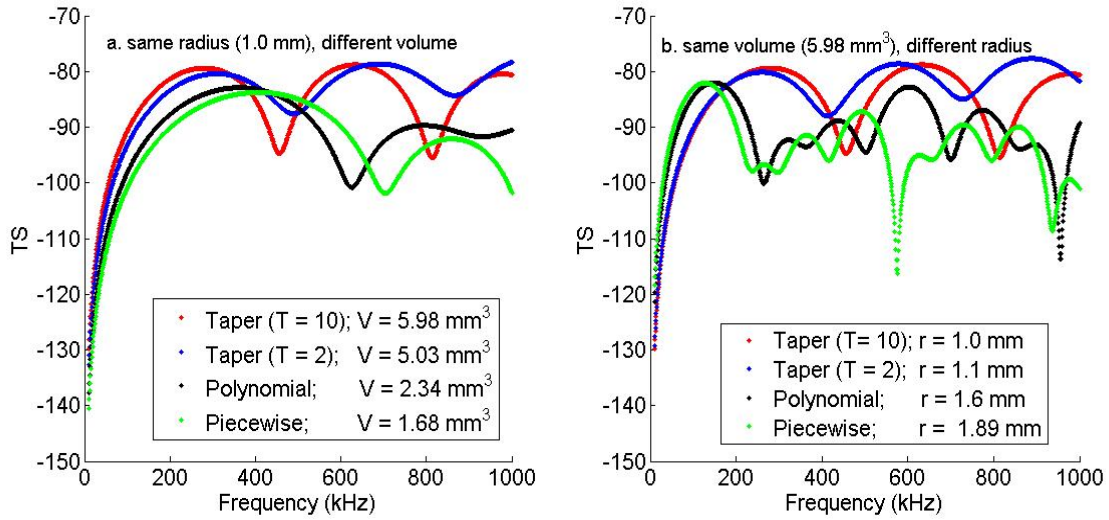

Fig. 14. TS calculated as a function of frequency for an individual krill with mean length, *g*, and *h* values measured from the Bering Sea. Calculations were made for an animal with broadside incidence and polynomial shape. a.) Constant radius (r = 1 mm) used for each euphausiid shape but varying volume. b.) Constant volume used for each shape but varying radius (Taper (T = 10) r = 1 mm; Taper (T = 2) r = 1.1 mm; polynomial r = 1.6 mm; piecewise r = 1.89 mm).

B. Animal length

Since the sixth degree polynomial was the preferred shape function, TS calculations made throughout the rest of the study will use this equation. Observed length, width, *g* and *h* measurements were used to calculate TS at 120 kHz for every individual animal. Overall, TS increased with animal length and a wide range in TS existed for each length measurement (Figure 15).

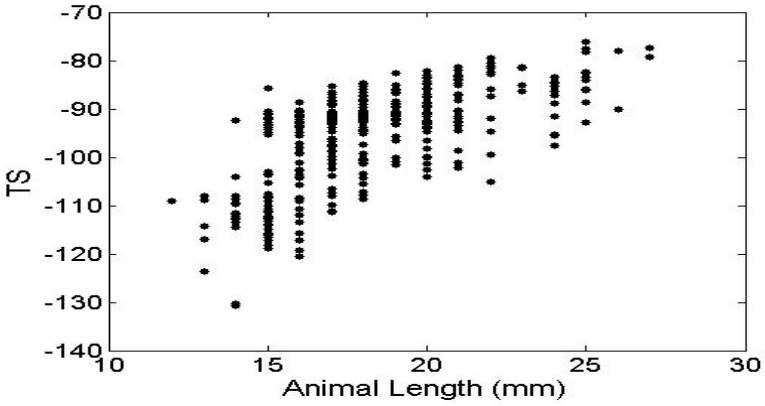

Fig. 15. TS calculated for each individual euphausiid collected from the Bering Sea (N = 380) using the measured length, width, *g*, and *h*, the polynomial shape function, a frequency of 120 kHz, and a broadside orientation.

C. Material properties

TS as a function of frequency was evaluated for many *g* and *h* measurements including the minimum, mean, and maximum values from Bering Sea euphausiids, as well as measurements of euphausiids in other studies. Each calculation of TS was made with either *g* or *h* varying while other model parameters were held constant at the mean values observed for Bering Sea specimens (Table 4) and at broadside incidence using the polynomial shape function. TS was also calculated for all combinations of minimum, maximum, and mean *g* and *h* values. For all combinations of *g* and *h*, the differences in TS away from the TS estimated using g_{mean} and h_{mean} are presented (Table 6). The maximum *h* value and maximum *g* value produced the largest TS estimates, but the minimum *h* and minimum *g* value did not produce the minimum TS estimates. Instead, a combination of the average *h* and minimum *g* produced the smallest TS estimates, while a combination of average *g* and minimum *h* produced the next lowest TS estimates.

Table 6. TS estimates were calculated by maintaining mean parameters and altering either *g* or *h* separately. This table gives the difference in TS values away from the TS estimate using mean parameters (i.e .difference in TS away from g_{mean} or h_{mean}). Material properties used from other studies are as follows: $g_{Greenlaw\ and\ Johnson}$=1.050, $g_{Køgeler}$=1.062, h_{Foote}=1.0279, $h_{Køgeler}$=1.031, and $h_{Chu\ and\ Wiebe}$=1.048. Mean length was used in calculations for an animal at broadside incidence with a polynomial shape.

g	h	ΔTS
g_{min}	h_{min}	-7.3
	h_{mean}	-11.2
g_{mean}	h_{min}	-1.8
	h_{max}	+2.9
	h_{Foote}	+6.0
	$h_{Køgeler}$	+6.6
	$h_{Chu\ and\ Wiebe}$	+9.1
g_{max}	h_{mean}	+6.2
	h_{max}	+7.7
$g_{Greenlaw\ and\ Johnson}$	h_{mean}	+7.7
$g_{Køgeler}$	h_{mean}	+9.3

Higher *g* and *h* values resulted in larger TS estimates regardless of frequency. TS at 120 kHz (broadside incidence, polynomial shape, mean euphausiid length) increased as *g* increased with *h* constant and as *h* increased with *g* constant, although not linearly (Figure 16).

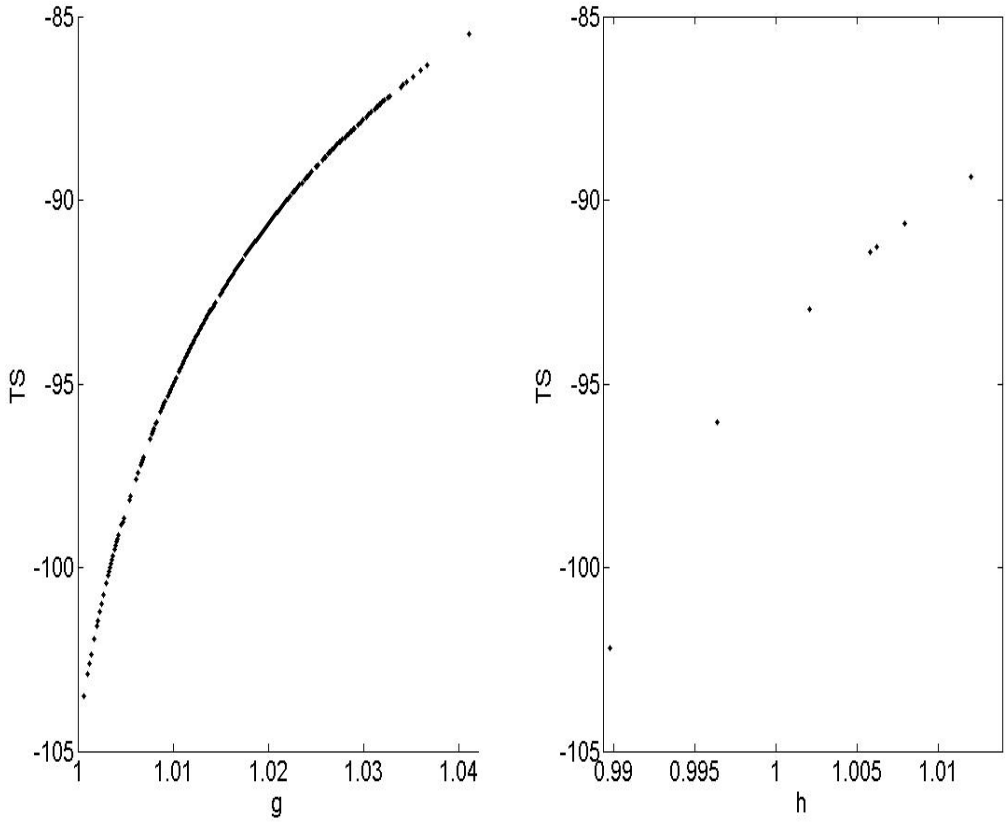

Fig. 16. a.) TS estimates as a function of *g* (other parameters: mean length, mean *h*, 120 kHz, broadside incidence, polynomial shape). b.) TS estimates as a function of *h* (other parameters: mean length, mean *g*, 120 kHz. broadside incidence, polynomial shape). Measurements of *h* are made on groups of animals, so there are fewer observations than shown in Fig 16a.

The relationship between *g* and *h* is difficult to evaluate since *g* is measured on individual animals and *h* is measured on groups of animals. However, there was no significant correlation between average *g* and *h* for Bering Sea euphausiids at each MT station where both properties were measured ($r = -0.22$, $p = 0.59$, $n = 8$). A scatterplot between *g* and *h* showed no strong relationship (Figure 17).

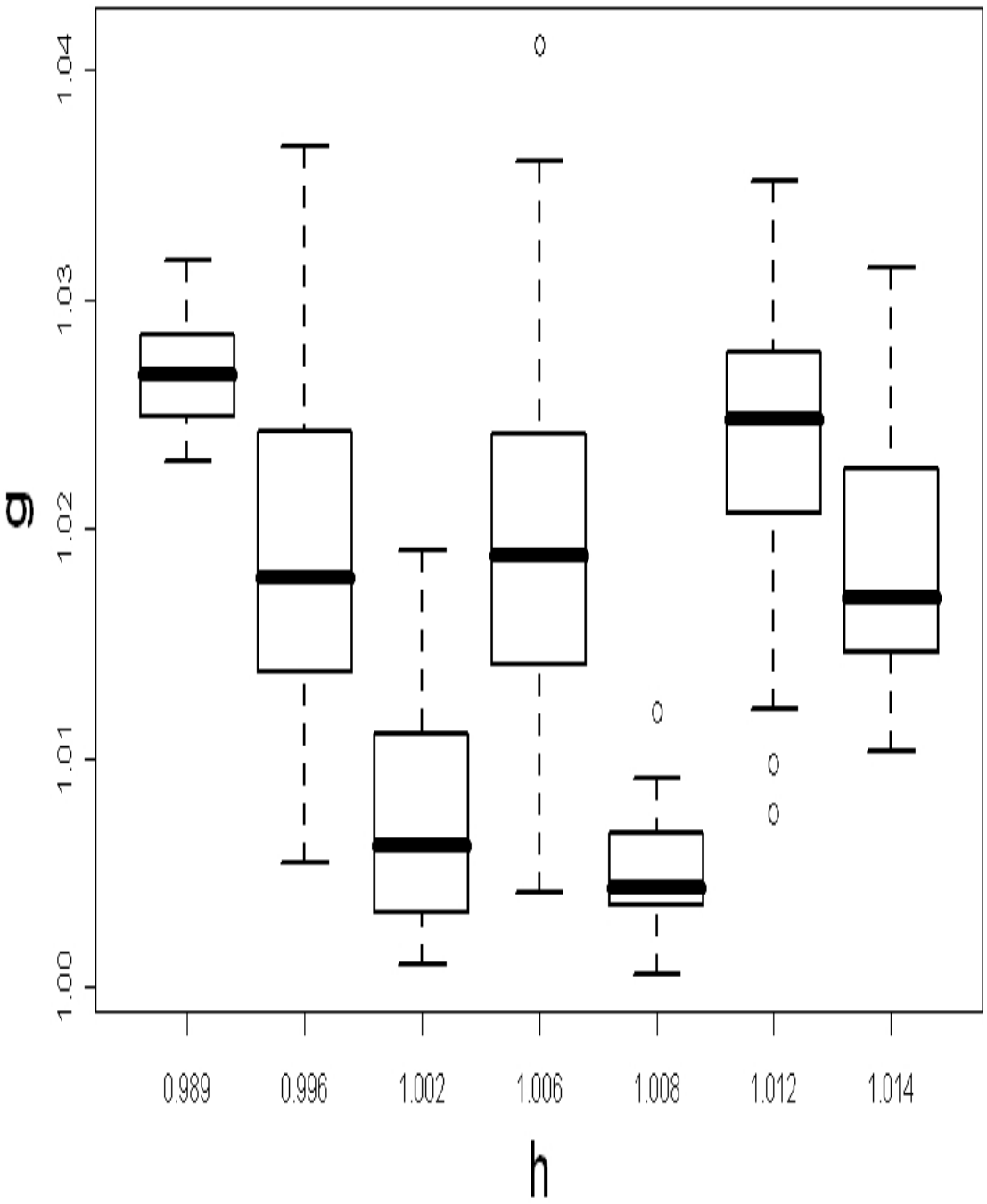

Fig. 17. Scatter plot of both material properties. No correlation between the two properties is indicated.

Extreme values of g and h can produce a wide range in TS estimates. For example, when keeping every other parameter constant and only examining the effects of g values from the Bering Sea on TS estimates, there was a 17.4 dB difference in the estimated TS value (g_{min} = 1.001 produced a TS value of -102.9 dB whereas g_{max} = 1.041 produced a TS value of -85.5 dB). Although not as great, there was also a difference in the TS estimate (4.7 dB) between the minimum and and maximum h value when all other parameters were kept constant (h_{min} = 0.9898 produces a TS value of -93.5 dB and h_{max} = 1.014 produced a TS value of -88.8 dB). Even though extreme values of material properties influence TS estimates, a more realistic description of TS variation due to material properties is given by examining variation of TS with R, since it is a function of both g and h (Table 7). The largest dB difference between MTs is 10.6 dB, and that the difference in average TS between East and West was only 2 dB (East TS = -87.7 dB;West TS = -89.7 dB).

Table 7. The average reflection coefficients (R) and associated standard deviations calculated for each MT. R was not calculated for MT06 because there was no h value collected for that location. Calculations were made using the R value from each MT, the mean length, at 120 kHz and broadside incidence.

MT	R	sd	Avg TS
1	0.007	0.001	-96.2
2	0.005	0.002	-99.5
3	0.008	0.006	-94.3
4	0.011	0.002	-91.3
5	0.018	0.003	-87.5
7	0.008	0.001	-94.2
8	0.017	0.004	-87.6
9	0.014	0.003	-88.8

Assuming the animal is at broadside incidence with a polynomial shape, the the estimated TS calculated at 120 kHz range from -103.8 dB to -91.8 dB (Table 8).

Table 8. The average TS of all animals measured from MT01 along with the corresponding density (animals/mm^3) estimate. Measured lengths, mean material properties, broadside incidence, and a polynomial shape were the default setting used when a particular parameter was varied.

	18 kHz		**38 kHz**		**70 kHz**		**120 kHz**		**200 kHz**	
ORIENTATION										
	TS	**N**	**TS**	**N**	**TS**	**N**	**TS**	**N**	**TS**	**N**
broadside	-122.8	3.5E03	-110.0	2.5E03	-99.6	1.7E03	-91.0	8.0E02	-84.3	2.4E02
N(45.3,30.4)	-123.6	4.2E03	-113.3	5.3E03	-108.9	1.4E04	-107.8	3.8E04	-114.5	2.5E05
N(11,4)	-122.9	3.6E03	-110.2	2.6E03	-100.6	2.1E03	-94.0	1.6E03	-94.3	2.3E03
head-on	-124.3	4.9E03	-115.7	9.3E03	-111.2	2.4E04	-115.4	2.2E05	-122.1	1.4E06
LENGTH										
Mean length	-123.6	4.1E03	-110.7	2.9E03	-100.3	2.0E03	-91.7	9.3E02	-85.0	2.8E02
measured lengths	-122.8	3.5E03	-110.0	2.5E03	-99.6	1.7E03	-91.0	8.0E02	-84.3	2.4E02
SHAPES										
taper (T=10)	-115.8	7.0E02	-103.0	5.0E02	-92.8	3.5E02	-84.7	1.8E02	-79.4	7.6E01
taper (T=2)	-118.5	1.3E03	-105.6	9.2E02	-95.4	6.3E02	-87.0	3.2E02	-81.1	1.1E02
polynomial	-122.8	3.5E03	-110.0	2.5E03	-99.6	1.7E03	-91.0	8.0E02	-84.3	2.4E02
piecewise	-115.4	6.3E02	-102.6	4.6E02	-92.7	3.4E02	-85.3	2.2E02	-82.3	1.5E02
MATERIAL PROPERTIES										
measured values	-127.2	9.5E03	-109.3	2.1E03	-99.2	1.5E03	-91.4	8.7E02	-86.8	4.2E02
uniform over measured ranges	-127.4	1.0E04	-114.3	6.8E03	-104.5	5.1E03	-96.4	2.7E03	-88.7	6.5E02
minimum reflectivity	-135.6	6.6E04	-122.7	4.7E04	-112.4	3.2E04	-103.8	1.5E04	-97.1	4.5E03
maximum reflectivity	-123.7	4.2E03	-110.8	3.0E03	-100.4	2.0E03	-91.8	9.6E02	-85.1	2.8E02
Foote 1990	-113.9	4.5E02	-101.0	3.2E02	-90.7	2.1E02	-82.1	1.0E02	-75.3	2.9E01
Chu and Wiebe 2005	-119.7	1.7E03	-106.8	1.2E03	-96.4	8.1E02	-87.8	3.8E02	-81.1	1.1E02

Another option when examining a more realistic range in TS estimates (as opposed to the extreme values), is to calculate the TS using the mean *g* and *h* values and to also calculate the TS using +2 SE for both *g* and *h* (Figure 18). This method produces a small range in TS values (~ 4 dB), although the orientation is different. Previous calculations used broadside incidence and this calculation used Lawson *et al.*'s (2006) orientation of N(0,27.3).

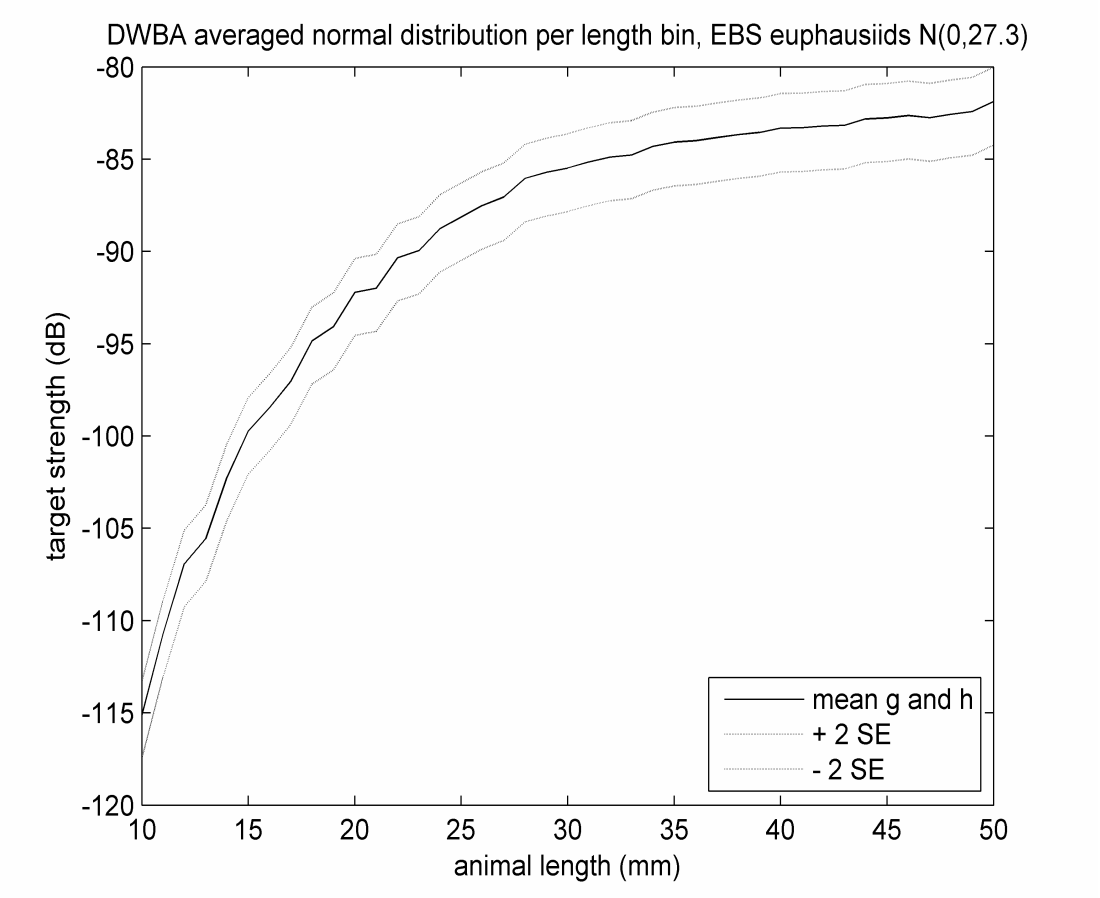

Fig. 18. TS was calculated using the mean *g* and *h* along with ± 2 SE *g* and *h* values.

D. Animal orientation and curvature

Animal curvature and orientation were evaluated for their influences on TS estimates. The average radius of curvature for the euphausiids examined was $\rho_c = 3.3L$. Assuming that ρ_c remains constant for all euphausiids, only one value of ρ_c was applied

for all animals instead of having a different ρ_c value for each individual euphausiid. Stanton *et al.* (1993) measured euphausiid curvature to be 3L, although they also showed that when backscattering cross-sections are averaged over a range of angles then they are nearly independent of ρ_c when $\rho_c \geq 2L$ (which is true in this study since 3.3L is greater than 2L). We still evaluated the TS using both 3.3L and 3L as the curvature to determine if there were any numerical differences and found that there was no difference in the TS estimate between using either curvature value.

Across a range of frequencies, orientation impacted on TS estimates made using various distributions of euphausiid orientation reported by other studies (Figure 19).

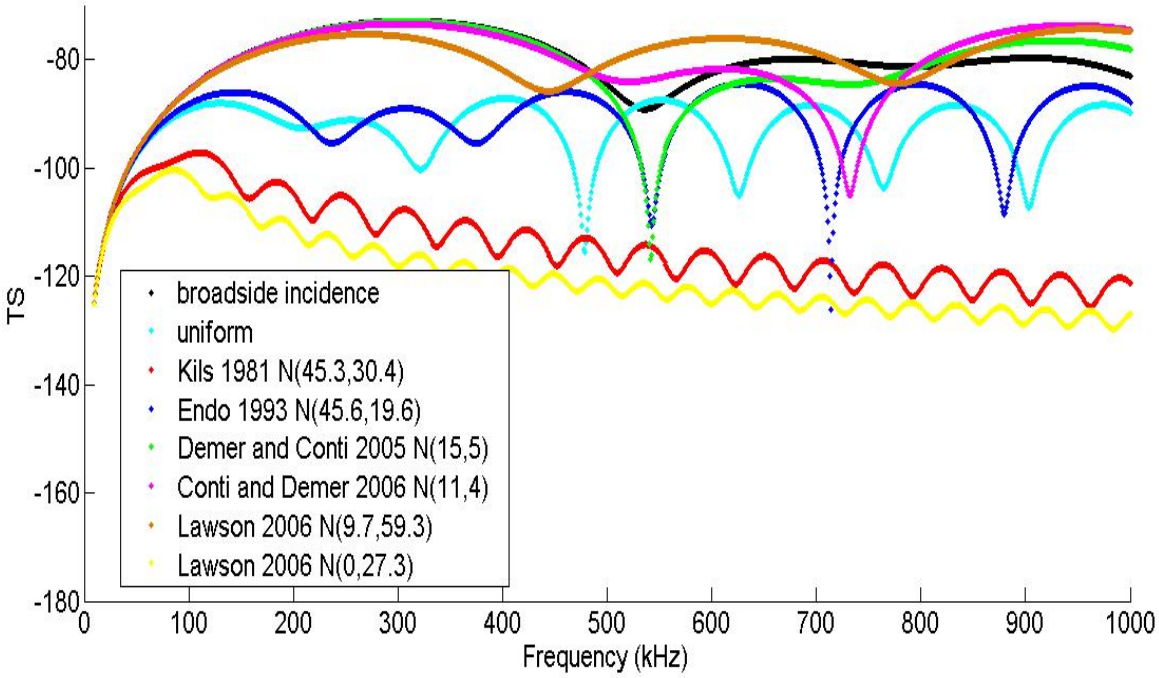

Fig. 19. TS as a function of frequency. Calculations made for several orientation distributions: broadside incidence, uniform, $N(\theta,\sigma_\theta)=N(45.3,30.4)$ from Kils (1981), $N(\theta,\sigma_\theta)=N(45.6,19.6)$ from Endo (1993), $N(\theta,\sigma_\theta)=N(15,5)$ from Demer and Conti (2005), and $N(\theta,\sigma_\theta)=N(11,4)$ from Conti and Demer (2006). The mean length and material properties were used to calculate the TS with a polynomial shaped euphausiid.

Polynomial shape, mean length, and mean material properties were used compute TS at each combination of orientation and frequency. Broadside incidence produced the largest TS values and the least amount of peaks and nulls across the range of frequencies.

Expectantly, orientation distributions near broadside incidence (N(15,5) from Demer and Conti, 2005 and N(11,4) from Conti and Demer, 2006) produced TS estimates similar to those produced when the animal was oriented at broadside incidence. In fact, the TS calculation were almost identical for low frequencies where scattering is governed by Rayleigh laws. Under a geometric scattering pattern (higher frequencies), the TS estimates produced the orientation distributions from Demer and Conti, 2005 and Conti and Demer, 2006 deviated slightly from the TS estimate produced at broadside incidence. The euphausiids described by Kils' (1981) orientation distribution are not horizontal in the water column and are at an angle (45.3º) with a large standard deviation (30.4); consequently, this orientation distribution produced the lowest TS estimates.

TS was also calculated for all incidence angles at four common echosounder frequencies: 18 kHz, 38 kHz, 120 kHz, and 200 kHz (Figure 20) for a euphausiid with a polynomial shape, mean length, and mean material properties. At the lowest frequency (18 kHz), TS was weakest and least sensitive to orientation; meanwhile, at the highest frequency (200 kHz), TS was greatest and had the largest difference in TS as euphausiid orientation shifted from broadside to end-on.

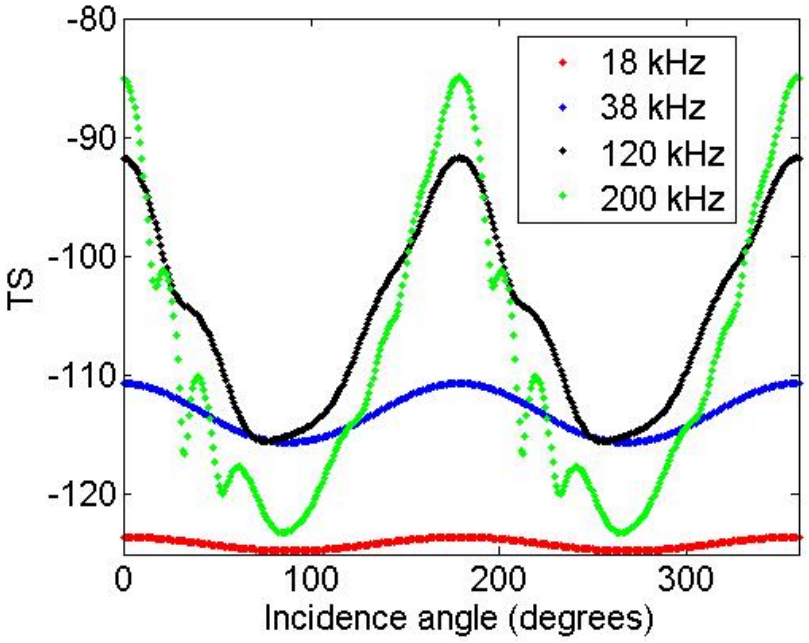

Fig. 20. TS calculated for all incidence angles (in degrees). Results from different frequencies (18 kHz, 38 kHz, 120 kHz, 200 kHz) are compared. Polynomial shape and mean length and material properties were used to calculate the TS.

E. Estimates of numerical density

Using acoustic survey data and the results of the DWBA model modeling, the acoustically-estimated abundance (numerical density) of krill in the water column was calculated for several locations and compared with net estimates. Average TS and numerical density estimates for MT01, MT03, the East, and the West were calculated at 120 kHz and 200 kHz (Table 9).

Table 9. The average TS (dB) and euphausiid numerical density (animals m^{-3}) calculated for MT01, MT03, the East, and the West. Numerical density measurements were calculated from volume backscattering strengths. Acoustic data is not from the same specific location as the animals were collected from due to shallow net tows, but are from the same (or nearby) station location and near-surface waters. TS was estimated assuming the animal was at broadside incidence, had a polynomial shape, and using the mean length.

	120 kHz			200 kHz		
	Avg TS	S_v	N	Avg TS	S_v	N
MT01	-91.4	-62.0	869	-86.8	-60.6	420
MT03	-105.7	-66.6	8,190	-98.8	-63.3	3,486
East	-87.7	-62.5	330	-82.2	-60.2	159
West	-89.7	-65.0	299	-86.3	-62.5	240

Volume backscattering strengths (S_v) at 120 kHz were available for two locations (MT01 and MT03) where we had nearly coincident nighttime net tow collections of animals for material property measurements and daytime estimates of s_v and euphausiid density from net tows. MT03 had a larger numerical density estimate than MT01 (Table 9). Smith *et al.* (in press) showed that there spatial variation in euphausiid material properties led to a distribution in *g* and *h* between the East and West sides of the study site. S_v values were

not measured at the exact location of the nighttime MTs , however, S_v data exist within the East and West regions. After averaging the S_v measurements in the linear domain for the East and West regions, the observed data on animal length, width, *g*, and *h* for both regions were used to calculate TS values. The numerical density of euphausiids was then calculated for both regions and the results showed that there was little difference in acoustic estimates of animal abundances between the East and West region (Table 9). The difference in TS between regions was 2 dB while the difference in observed S_v was 2.5 dB. Numerical densities were calculated again, but the TS value was kept constant for both regions (-88.7 dB) and the observed S_v values were used. In this case, where the average TS was kept constant for both regions and the S_v values differed by 2.5 dB, the results showed a 2X difference in numerical density where the East had 420 animals m^{-3} and the West had 230 animals m^{-3}.

Species composition and numerical densities were calculated for the zooplankton collected by the net tows. Comparisons between the numerical density of the net tows and estimated from acoustic data were made for MT01 and MT03. The numerical density of MT01 from the net tow was 13.3 animals m^{-3} which is significantly smaller than the estimate made from acoustic data (Table 9). Likewise, the numerical density estimate from the net tow for MT03 (a value of 37.7 animals m^{-3}) was much smaller than the numerical density value estimated from acoustic data. In both derivations of the numerical density value, the number of animals within a cubic meter of water was still greater at MT03 compared to MT01.

Numerical densities were calculated for nine daytime Methot tows using observed S_v, a distribution of measured euphausiid lengths, and applying *g* and *h* values for the East and West regions that corresponded to the average R value for each region. The first six daytime tows (DTs) were a part of the East region and DTs seven through nine were a part of the West region. Calculations were made at 120 kHz for euphausiids at broadside incidence with a polynomial shape. The numerical densities derived from acoustic data were also compared to numerical densities estimated from the net tows, in which the acoustic estimates were larger than the net tow estimates (Figure 21).

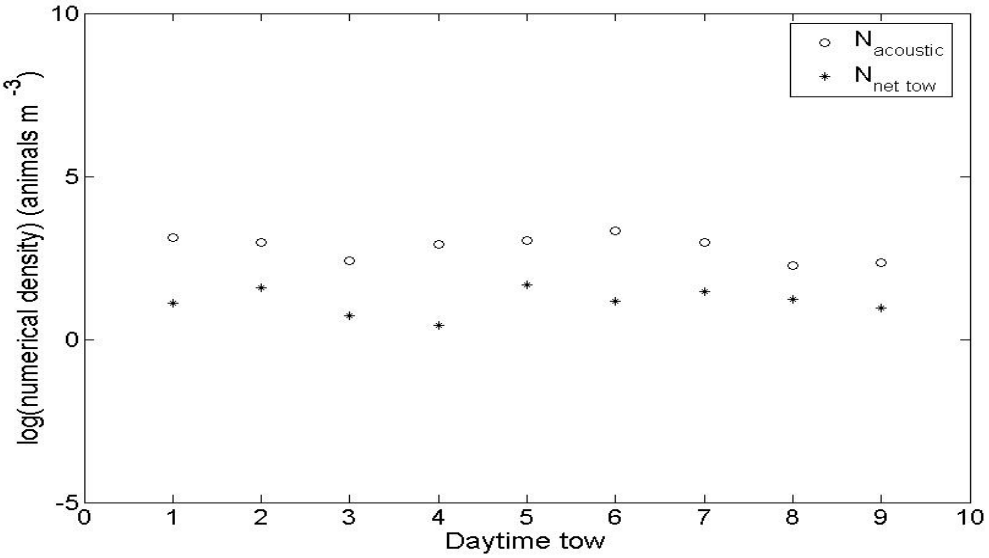

Fig. 21. Numerical densities derived from acoustic data ($N_{acoustic}$) were calculated for nine daytime tows (DT) using observed S_v data and average length data collected from the daytime tow. The *g* and *h* values for the East and West regions from the nighttime MTs that corresponded to the average R values were applied to each daytime tow (East = DT1-6; West = DT7-9). Calculations were made at 120 kHz, at broadside incidence, and assuming the euphausiids were polynomial shaped. Numerical densities from the net tows ($N_{net\ tow}$) is also shown. Numerical densities are given in the logarithmic scale.

F. Comparison to other models

When the animal was near broadside incidence (i.e. N(11,4) from Conti and Demer, 2006), the TS calculations were almost identical (Figure 22).

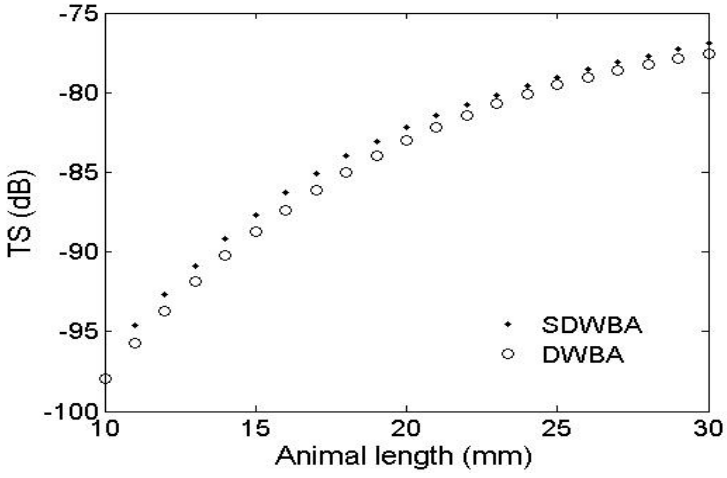

Fig. 22. TS estimates were calculated using both the DWBA model and the SDWBA model. Comparisons were made for animals near broadside incidence with an orientation distribution of N(11,4) (Conti and Demer, 2006) and material property values of *g* = 1.0357 and *h* = 1.0279.

IV. Discussion

A DWBA model was parameterized using observed physical and material properties from live specimens to calculate the TS of Bering Sea euphausiids. In order to examine the effect of variability in the different scattering model inputs, several assumptions were made. For instance, there was no strong species effect on *g* (Smith *et al*., in press) therefore measurements of animal characteristics were combined for all euphausiid species. Most studies define euphausiid shape using one function. For the majority of our calculations, the shape function used in the TS model is the polynomial function. Orientation distributions were not measured during this study, so several orientation distributions reported elsewhere (Kils, 1981; Endo, 1993; Demer and Conti, 2005; Conti and Demer, 2006) were used. The average TS was computed for all animals in MT01, MT03, the East, and the West. The numerical density of euphausiids was then calculated for each of these areas using observed S_v and information from the net capture. Numerical densities were also similarly calculated for nine daytime tows.

A. Effect of shape

The sixth degree polynomial model presented in this study is based upon empirical measurements of Bering Sea euphausiids and more realistically portrays the animal as being asymmetrical from head to tail. Unlike the piecewise function, it does not contain inflection points or abrupt changes in the animal width. The various shape equations produced significantly different TS estimates with the taper function (T=10) estimating TS to be 7 dB and 9.6 dB higher than the TS produced by the polynomial and piecewise function. One possible explanation for the TS difference between shape functions is the change in animal volume for the same animal length. The polynomial shape function predicts a smaller TS (because of the smaller volume) for an animal of a given length, when all other factors remain constant (Figure 13). Since the taper function produces larger TS values compared to the polynomial shape, it means fewer animals per m^3 would be estimated for a given S_v than if the polynomial was used.

Differences in TS between the taper and realistic shape functions (piecewise and polynomial) also occurred when animals had equivalent volumes, suggesting that the influence of shape is important. The more realistic shape functions produced smaller TS

values at high frequencies(> 100 kHz). Because of the differences in animal shape, we acknowledge that the TS estimates for Bering Sea krill in this study will be lower than those produced with models that use the taper function.

B. Effect of length

Even though the differences in TS were not large when using the mean length versus the measured length, there is still a clear relationship between animal length and their estimated TS values (Figure 15). Length is an important factor when calculating TS, however, material properties are even more important when estimating TS for Bering Sea euphausiids. Even so, length and width measurements should be made whenever possible in order to more accurately parameterize scattering models for future studies since both measurements are easy to collect.

C. Effect of material properties

Both *g* and *h* were shown to increase TS as *g* or *h* diverged from unity, with TS varying by 15-20 dB, although this relationship was not linear (Figure 16). Density contrast had a greater influence on the TS estimate compared to sound speed contrast, although this may be the result of the measured *g* being more variable than measured *h*. The range of TS calculated using the highest and lowest *g* and *h* values measured in the Bering Sea was smaller than the range of TS calculated using range of both Bering Sea measurements and values reported in the literature for other euphausiid taxa from other regions (Table 6). This demonstrated that taxon- and area- specific measurements of material properties help reduce and characterize uncertainty in model predictions.

Other studies report higher *g* and *h* values (Greenlaw and Johnson, 1982; Køgeler *et al*., 1987, Foote, 1990; Chu and Wiebe, 2005) so our analysis included these numbers. Greenlaw and Johnson (1982) provide a *g* value of 1.050 for krill and the corresponding TS value was -84.0 dB (keeping all other variables constant). This was only 1.5 dB higher than the TS estimate using the largest *g* value (1.041) measured on euphausiids from the Bering Sea; however, it was 18.9 dB larger than the TS estimate using the smallest *g* value (1.001) measured on euphausiids from the Bering Sea. The highest *g* value presented by Køgeler *et al.* (1987) was 1.062 which generated a TS of -82.3 dB, which is 3.1 dB larger than the TS estimated using the largest *g* measured from the

Bering Sea, and 20.5 dB larger than the TS estimated from the smallest *g* observed. Although both *g* and *h* separately influence TS estimates, the combination of both *g* and *h* affects TS via the reflection coefficient. The range in *g* and *h* values used to determine the minimum and maximum reflection coefficient are more useful in determining a realistic range in TS values.

D. Effect of orientation

We did not measure the *in situ* orientation of Bering Sea euphausiids, so distributions of euphausiid orientations from other studies (Kils, 1981; Endo, 1993; Demer and Conti, 2005; Conti and Demer, 2006) were used to evaluate the effect on DWBA model predictions. Orientation has a large effect on model predictions of euphausiid TS, particularly at higher frequencies (Figure 19 and 20). As expected, broadside incidence produced the largest TS values (Figures 19) and animals swimming nearly horizontal (Demer and Conti, 2005 and Conti and Demer, 2006 orientation distributions) had TS estimates close to measurements made at broadside incidence. The large variation in TS calculated for individual euphausiids for all MTs (Figure 15) highlights the importance of having an orientation distribution relative to the specific animals being studied, although these observations are difficult to collect.

In situ orientation is likely to change throughout the day as euphausiids vertically migrate throughout the water column (Price, 1989). It would be ideal to incorporate the changes in orientation throughout the day into the DWBA model to more accurately predict the average TS and numerical density. If a relationship between orientation and time of day (or light availability, food availability, or other covariate) could be modeled for a given region, euphausiid orientation could be predicted and then applied to DWBA model estimates of TS.

E. Numerical density estimates

The traditional approach to estimating numerical densities of euphausiids is to use one TS value for the whole survey and calculate numerical density using observed S_v measurements. When the average TS was kept constant and only the S_v varied between the East and West regions, there was a factor of two difference in the estimated density of krill (4.2×10^2 animals m^{-3} in the East and 2.3×10^2 animals m^{-3} in the West). Using

measured *g*, *h*, and animal length values, this study calculated a separate average TS value for the East and West region. The same observed S_v values were used and produced similar numerical densities for both regions ($3.3x10^2$ animals m^{-3} in the East and $3.0x10^2$ animals m^{-3} in the West). This is due to the variation in material properties and animal lengths which caused the average TS to differ for the two regions. Variation in measured S_v values can result from either differences in animal densities or TS values of the scatterer. Since material properties can vary spatially (Smith *et al*., in press), the most accurate numerical density estimates would be calculated using material properties, animal lengths, and orientation of the animals for each new study site.

The numerical density estimates were similar between the East and the West region, which was unanticipated considering the spatial variation in material properties. This observation is unexpected considering that the average TS calculation for the East is 2dB higher than the average TS calculation for the West (Table 7). Since the East has the larger TS value, it would be expected that the East should have fewer euphausiids than the West; however, the numerical density estimates derived from the measured S_v values do not support this assumption. Instead, the numerical density estimates are roughly the same for both regions (Table 9). One explanation could be that the S_v measurements do not correspond to the same exact locations where the measured material properties were located.

By comparing the numerical density values calculated from the net tow catches and the acoustic derived value, the numerical density from the acoustic data is much larger for the two locations examined (MT01 and MT03). This observation is not uncommon considering euphausiids can swim away from nets.

Similar results were observed when comparing the numerical density estimates for the daytime tows (Figure 21); the numerical density estimates derived from acoustic data were also larger than the numerical density value estimated from the net tow. Overall the eastern daytime tows (DT1-6) had larger numerical density estimates compared to the western tows (DT7-9). Even though material properties were not measured specifically for the euphausiids in the daytime tows, we were able to apply *g* and *h* values observed from euphausiids from the nighttime tows to other areas that fit within the same East and

West regions. Since it is difficult to obtain all parameters at each study site, we suspect that this will become common practice in which material property measurements will be applied to other study sites in close proximity to where the material property measurements were collected.

F. Comparison to other models

TS calculations using a smooth tapered-bent cylinder (Stanton and Chu, 2000) produced higher estimates compared to results from the polynomial shape. This is partially because *g* and *h* measurements from Stanton and Chu's (2000) study were larger than the mean material properties used in this study. Even though there were additional undulations in the incidence angle versus TS pattern from the Chu and Stanton (2000) study (Figure 20 from this study compared to Figure 5 in Stanton and Chu's 2000 study), our overall results agreed with theirs. Both studies indicate that orientation has a large impact on TS estimates and that small changes in material properties can have a large difference in TS estimates. In particular, Stanton and Chu (2000) show that a small change of only 1 to 6% difference in the material properties leads to a fairly large (15 dB) difference in TS.

The DWBA model was used instead of the SDWBA model (Demer and Conti, 2003a) because it has been shown to accurately predict TS for euphausiids which swim mostly horizontally (McGehee *et al.*, 1998), orientations at which euphausiids commonly swim (Demer and Conti, 2005; Conti and Demer, 2006). Although the SDWBA model can also accurately predict TS for animals near horizontal incidence, it is easier to implement variations of the different parameters into the DWBA model. Under the same assumption, the DWBA model has been continuously used even after the development of the SDWBA model for euphausiids as well as other animal types (Lawson *et al*, 2006; Amakasu and Furusawa, 2006; Lee *et al.,* 2008).

V. Recommendations

Ideally the physical properties, material properties, and *in situ* orientations should be measured for a subsample of euphausiids from every study site. Each parameter has the potential to alter model predictions of euphausiid TS by as much as 20 dB, leading to

uncertainties in population estimates of up to two orders of magnitude. Regardless, there was still a large variation in TS estimates based on the measurements collected in Bering Sea euphausiids (Figure 15).

To reduce uncertainty in TS estimates, material properties should be measured for the specific zooplankton taxa being studied in the region of study, rather than applying the material property values observed for other taxa in other regions (commonly done due to a lack of material property data for many species). Using the appropriate physical and material properties observed for euphausiids from the Bering Sea, site-specific population estimates were made for two eastern MTs and nine daytime tows in both the East and West regions. Smith *et al.* (in press) showed that location had a significant effect on *g* measurements, although these differences were most likely the result of model parameters varying with geographic location. This suggests that acoustic surveys over large areas may need to measure scattering model inputs at multiple sites, particularly in regions where environmental or zooplankton characteristics vary greatly.

Several uncertainties are associated with the results from this study. Numerical density predictions of animals are likely overestimates as the inversion of S_v data assumes all scattering in the water column is from euphausiids. The model predictions of TS in this study are lower than previous studies, possibly due to the difference in shape functions. Numerical density estimates from other studies are likely an overestimate because they use the taper function which has a larger volume than the polynomial function described in this study (Chu *et al.*, 1993; Lawson *et al.*, 2006).

It is nearly logistically impossible to collect all parameters required to make the most accurate TS estimates (S_v data, length and material property measurements, orientation distributions, etc), so applying data to be used in different areas from where they were collected is practical. Several of the model parameters examined in this study should be investigated in more detail in any region where acoustic surveys are used to estimate animal abundance. Regardless, the improved parameterization of the DWBA model specific to Bering Sea euphausiids can be applied to future acoustic surveys in this region.

REFERENCES CITED

Adams, C.F., Pinchuk, A.I., and Coyle, K.O. (2007). "Seasonal changes in the diet composition and prey selection of walleye pollock (Theragra chalcogramma) in the northern Gulf of Alaska." Fisheries Research 84, 378-389.

Adams, C.F., Foy, R.J., Kelley, J.J., and K.O.Coyle. (2009). "Seasonal changes in the diel vertical migration of walleye pollock (*Theragra chalcogramma*) in the northern Gulf of Alaska." Environ. Biol. Fish. **86**, 297-305.

Amakasu, K. and Furusawa, M. (2006). "The target strength of Antarctic krill (*Euphausia superba*) measured by the split-beam method in a small tank at 70 kHz." ICES J. of Mar. Sci. **63**, 36-45.

Anderson, V.C. (1950). "Sound scattering from a fluid sphere," J. Acoust. Soc. Am. **22**(4), 426-431.

Bailey, K.M. (1989). "Interaction between the vertical distribution of juvenile walleye pollock *theragra chalcogramma* in the eastern Bering Sea, and cannibalism." Mar. Ecol. Progr. Ser. **53**, 205-213.

Brierley, A.S., and Watkins, J.L. (1996). "Acoustic targets at South Georgia and the South Orkney Islands during a season of krill scarcity," Mar. Ecol. Prog. Ser. **138**, 51-61.

Brodeur, R.D., Wilson, M.T., Ciannelli, L., Doyle, M. and Napp, J.M. (2002). "Interannual and regional variability in distribution and ecology of juvenile pollock and their prey in frontal structures of the Bering Sea," Deep-Sea Res. II. **49**, 6051-6067.

Campbell, R.W., and Dower, J.F. (2003). "Role of lipids in the maintenance of neutral bouyancy by zooplankton," Mar. Ecol. Prog. Ser. **263**, 93-99.

Chu, D., Foote, K.G. and Stanton, T.K. (1993). "Further analysis of target strength measurements of Antarctic krill at 38 and 120 kHz: Comparison with deformed cylinder model and inference of orientation distribution." J. Acoust. Soc. Am. 93(5), 2985-2988.

Chu, D., and Ye, Z. (1999). "A phase-compensated DWBA representation of the bistatic scattering by weakly scattering objects: Applications to zooplankton," J. Acoust. Soc. Am. **106**, 1732-1743.

Chu, D., Wiebe, P. and Copley, N. (2000). "Inference of material properties of zooplankton from acoustic and resistivity measurements," ICES J. Mar. Sci. **57**, 1128-1142.

Chu, D., and Wiebe, P.H. (2005). "Measurements of sound-speed and density contrasts of

zooplankton in Antarctic waters," ICES J. Mar. Sci. **62**, 818-831.

Ciannelli, L., Brodeur, R.D., and Napp, J.M. (2004). "Foraging impact on zooplankton by age-0 walleye pollock (*Theragra chalcogramma*) around a front in the southeast Bering Sea," Mar. Biol. **144**, 515-525.

Conti, S.G. and Demer, D.A. (2006). "Improved parameterization of the SDWBA for estimating krill target strength." ICES J. of Mar. Sci. 63, 928-935.

Coyle, K.O., Hunt, Jr., G.L., M.B. Decker, and Weingartner, T.J. (1992). "Murre foraging, epibenthic sound scattering, and tidal advection over a shoal near St. George Island, Bering Sea," Mar. Ecol. Prog. Ser. **83**, 1-14.

Coyle, K.O., and Pinchuk, A.I. (2002). "The abundance and distribution of euphausiids and zero-age pollock on the inner shelf of the southeast Bering Sea near the inner front in 1997-1999," Deep-Sea Res. II. **49**, 6009-6030.

Coyle, K.O., Pinchuk, A.I., Eisner, L.B., and Napp, J.M. (2008). "Zooplankton species composition, abundance and biomass on the eastern Bering Sea shelf during summer: The potential role of water-column stability and nutrients in structuring the zooplankton community," Deep-Sea Res. II. **55**, 1775-1791.

Dagg, M.J., Clarke, M.E., Nishiyama, T. and Smith, S.L. (1984). "Production and standing stock of copepod nauplii, food items for larvae of the walleye pollock *Theragra chalcogramma* in the southeastern Bering Sea," Mar. Ecol. Prog. Ser. **19**, 7-16.

Decker, M.B., and Hunt, Jr., G.L. (1996). "Murre foraging at the frontal system surrounding the Pribilof Islands, Alaska," Mar. Ecol. Prog. Ser. **139**, 1-10.

Demer, D.A.and Conti, S.G. (2003a). "Reconciling theoretical versus empirical target strengths of krill: effects of phase variability on the distorted-wave Born approximation." ICES J. of Mar. Sci. **60,** 429-434.

Demer, D.A. And Conti, S.G. (2003b). "Validation of the stochastic distorted-wave Born approximation model with broad bandwidth total target strength measurements of Antarctic krill." ICES J. of Mar. Sci. **60,** 625-635.

Demer, D.A. And Conti, S.G. (2005). "New target-strength model indicates more krill in the Southern Ocean." ICES J. of Mar. Sci. **62,** 25-32.

Demer, D.A. and Conti, S.G. (2006). "Improved parameterization of the SDWBA for estimating krill target strength". ICES J. of Mar. Sci. **63,** 928-935.

Endo, Y. (1993). "Orientation of Antarctic krill in an aquarium." Nippon Suisan Gakkaishi, **59**(3), 465-468.

FAO (2009). The State of World Fisheries and Aquaculture 2008, Part 1. World review of fisheries and aquaculture. FAO Fisheries and Aquaculture Department, Viale delle Terme di Caracalla, 00153 Rome, Italy, 176 p. http://www.fao.org/docrep/ 011/i0250e/ i0250e00 .htm

Foote, K.G., Knudsen, H.P., Vestnes, G., MacLennan, D.N., and Simmonds, E.J. (1987). "Calibration of acoustic instruments for fish density estimates: a practical guide," ICES Coop. Res. Rep. 144.

Foote, K.G. (1990). "Speed of sound in Euphausia superba," J. Acoust. Soc. Am. **87**(4), 1405-1408.

Foote, K.G., Everson, I., Watkins, J.L., and Bone, D.G. (1990). "Target strengths of Antarctic krill (*Euphausia superba*) at 38 and 120 kHz," J. Acoust. Soc. Am. **87**(1), 16-24.

Foote, K.G., and Stanton, T.K. (2000). "Acoustical methods," ICES Zooplankton Methodology Manual, edited by eds. R. Harris, P. Wiebe, J. Lenz, H. Skjoldal, and M. Huntley (Academic London), pp. 223-258.

Forman, K.A. and Warren, J.D. (2009). "Variability in the density and sound-speed of coastal zooplankton and nekton," ICES J. Mar. Sci. **67**(1), 10-18. doi:10.1093/icesjms/fsp217

Gorska, N., Ona, E. and Korneliussen, R. (2005). "Acoustic backscattering by Atlantic mackerel as being representative of fish that lack a swimbladder. Backscattering by individual fish." ICES J. of Mar. Sci. **62,** 984-995.

Greenblatt, P. (1981). "Sources of acoustic backscattering at 87.5 kHz," J. Acoust. Soc. Am. **70**(1), 134-142.

Greenlaw, C.F. (1977). "Backscattering spectra of preserved zooplankton," J. Acoust. Soc. Am. **62**, 44-52.

Greenlaw, C.F., and Johnson, R.K. (1982). "Physical and acoustical properties of zooplankton," J. Acoust. Soc. Am. **72**(6), 1706-1710.

Hagen, W., Van Fleet, E.S., and Kattner, G. (1996). "Seasonal lipid storage as overwintering strategy of Antarctic krill," Mar. Ecol. Prog. Ser. **134**, 85-89.

Harris, R.P., Wiebe, P.H., Lenz, J., Skjoldal, H.R. and M. Huntley (Eds.) (2000). Zooplankton Methodology Manual. Elsevier Academic Press, London, UK. "Chapter 3.3: Factors influencing mesozooplankton samples." pp. 67-72.

Hatch, S.A. And G.A. Sanger. (1992). “Puffins as samplers of juvenile pollock and other forage fish in the Gulf of Alaska.” Mar. Ec. Prog. Ser. **80**, 1–14.

Honkalehto, T., Patton, W., de Blois, S., and Williamson, N. (2002). “Echo integration-trawl survey results for walleye pollock (*Theragra chalcogramma*) on the Bering Sea shelf and slope during summer 1999.” U.S. Department of Commerce, NOAA Technical Memorandum NMFS-AFSC-125, 66 p.

Honkalehto, T., Jones, D., McCarthy, A., McKelvey, D. Guttormsen, M., Williams, K. and Williamson, N. (2009). Results of the Echo Integration-Trawl Survey of Walleye Pollock (*Theragra chalcogramma*) on the U.S. and Russian Bering Sea Shelf in June and July 2008. U.S. Department of Commerce, NOAA Technical Memorandum NMFS-AFSC-194, 56 p. http://www.afsc.noaa.gov/Publications/AFSC-TM/NOAA-TM-AFSC-194.pdf

Ianelli, J.N., Barbeaux, S., Honkalehto, T.; Kotwicki, S.; Aydin, K. and Williamson, N. (2008). “Assessment of the walleye pollock stock in the eastern Bering Sea,” p. 47-136 in “Stock Assessment.” NPFMC Bering Sea and Aleutian Islands Stock Assessment and Fishery Evaluation (SAFE) document. 605 W. 4th Ave., Anchorage, AK 99501.

Iida, T. and Saitoh,S.I. (2007). “Temporal and spatial variability of chlorophyll concentrations in the Bering Sea using emperical orthogonal function (EOF) analysis of remote sensing data,” Deep Sea Res. II. **54,** 2657-2671.

Jones, B.A., Lavery, A.C., and Stanton, T.K. (2009). “Use of the distorted wave Born approximation to predict scattering by inhomogeneous objects: Applications to squid.” J. Acoust. Soc. Am. **125**, 73-88.

Kang, M., Furusawa, M., and K. Miyashita. (2002). “Effective and accurate use of difference in mean volume backscattering strength to identify fish and plankton.” ICES J. Mar. Sci. **59**, 794-804.

Kang, D., Iida, K., Mukai, T. and Hwang, D. (2004). “Acoustic target strength of Japanese common squid, Todarodes pacificus, and important parameters influencing its TS: swimming angle and material properties.” in *OCEANS'04 MTS/IEEE/TECHNO-OCEAN'04*, 364-369.

Kasatkina, S.M., Gross, C., Emery, J.H., Takao, Y., Litvinov, F.F., Malyshko, A., Shnar, V.N., and O.A.Berezhinsky. (2004). “A comparison of net and acoustic estimates of krill density in the Scotia Sea during the CCAMLR 2000 Survey.” Deep-Sea Res. II. **51**, 1289-1300.

Kils, U. (1981). “The swimming behavior, swimming performance and energy balance of

Antarctic krill, Euphausia superba." BIOMASS Sci. Ser. No.3.

Køgeler, J.W., Falk-Petersen, S., Kristensen, Å., Pettersen, F. and Dalen, J. (1987). "Density- and sound speed contrasts in sub-Arctic zooplankton," Polar Biol. **7**, 231-235.
Methot, R.D. (1986). "Frame trawl for sampling pelagic juvenile fish," Southwest Fisheries Center, CalCOFI Rep. 27: 267-268.

Lang, G.M., Brodeur, R.D., Napp, J.M. and R. Schabetsberger. (2000). "Variation in groundfish predation on juvenile walleye pollock relative to hydrographic structure near the Pribilof Islands, Alaska." ICES J. Mar. Sci. **57**, 265-271.

Lang, G.M., Livingston, P.A., and K.A. Dodd. (2005). "Groundfish food habits and predation on commercially important prey species in the eastern Bering Sea from 1997 through 2001." U.S. Dep. Commer., NOAA Tech. Memo. NMFS-AFSC-158, 230p.

Lavery, A.C., Stanton, T.K., McGehee, D.E., and D. Chu. (2002). "Three-dimensional modeling of acoustic backscattering from fluid-like zooplankton." J. Acoust. Soc. Am. **111**(3), 1197-1210.

Lawson, G.L., Wiebe, P.H., Ashjian, C.J., Chu, D. and T.K. Stanton. (2006). "Improved parameterization of Antarctic krill target strength models." J. Acoust. Soc. Am. **119**(1), 232-242.

Lawson, G.L., Wiebe, P.H., Stanton, T.K., and C.J. Ashjian. (2008). "Euphausiid distribution along the Western Antarctic Peninsula-Part A: Development of robust multi-frequency acoustic techniques to identify euphausiid aggregates and quantify euphausiid size, abundance, and biomass." Deep-Sea Res. Part 2. Topical studies in oceanography. **55**, 412-431.

Lee, K., Mukai, T., Lee, D. and Iida, K. (2008). "Verification of mean volume backscattering strength obtained from acoustic Doppler current profiler by using sound scattering layer." Fisheries Science. **74**, 221-229.

Livingston, P.A. (1991). "Walleye pollock,"Groundfish food habits and predation on commercially important prey species in the eastern Bering Sea, 1984-1986. edited by P.A. Livingston. U.S. Dep. Commer., NOAA Tech. Memo. NMFS-F/NWC-207.

Mauchline, J. (1980). "Measurement of body length of Euphausia superba Dana," BIOMASS Handbook No. 4, pp. 4-9.

McKelvey, D.R. And C.D. Wilson. (2006). "Discriminant classification of fish and zooplankton backscattering at 38 kHz and 120 kHz." Transactions of the Am. Fish. Soc. **135**, 488-499.

Medwin, H. and C.S. Clay. (1998). Fundamentals of Acoustical Oceanography. Academic Press, San Diego, California.

Methot, R.D. (1986). "Frame trawl for sampling pelagic juvenile fish." National Marine Fisheries Service, Southwest Fisheries Center, CalCOFI Rep, Vol 27.

Morse, P.M. and K.U. Ingard. (1968). Theoretical Acoustics. Princeton University Press, Princeton, NJ.

Murphy, B.R. And D.W. Willis (Eds.) (1996). Fisheries Techniques, 2nd Edition. Published by American Fisheries Society. "Chapter 7: Active fish capture methods" pp. 193-220.

Miyashita, K. (2003). "Diurnal changes in the acoustic-frequency characteristics of Japanese anchovy (*Eugraulis japonicus*)_post-larvae "shirasu" inferred from theoretical scattering models." ICES J. of Mar. Sci. **60**, 532-537.

Price, H.J. (1989). "Swimming behavior of krill in response to algal patches: A mesocosm study." Limnol. Oceanogr. **34**(4), 649-659.

Reiss, C.S., Cossio, A.M., Loeb, V. and D.A. Demer. (2008). "Variations in the biomass of Antarctic krill (Euphausia superba) around the South Shetland Islands, 1996-2006." ICES J. Mar. Sci. **65**(4), 497-508.

Schabetsberger, R., Brodeur, R.D., Ciannelli, L., Napp, J.M. and Swartzman, G.L. (2000). "Diel vertical migration and interaction of zooplankton and juvenile walleye pollock (*Theragra chalcogramma*) at a frontal region near the Pribilof Islands, Bering Sea," ICES J. Mar. Sci. **57**(4), 1283-1295.

Simmonds, J., and MacLennan, D. (2005). Fisheries Acoustics: Theory and Practice. 2nd ed. Blackwell Science Ltd., Oxford, UK, 437 p.

Sinclair, E. (1994). "Prey selection by northern fur seals (*Callorhinus ursinus*) in the eastern Bering Sea," Fish. Bull. **92**(1), 144-156.

Sogard, S.M. And Olla, B.L. (1994). "The potential for intracohort cannibalism in age-0 walleye pollock, *Theragra chalcogramma*, as determined under laboratory conditions." Env. Biol. of Fishes. **39**, 183-190.

Springer, A.M., and Roseneau, D.G. (1985). "Copepod-based food webs: auklets and oceanography in the Bering Sea," Mar. Ecol. Prog. Ser. **21**, 229-237.

Springer, A.M. (1992). "A review: walleye pollock in the North Pacific-how much difference do they really make?" Fish. Ocean. **1**, 80-96.

Smith, S.L. (1991). “Growth, development and distribution of the euphausiids *Thysanoessa raschi* (M. Sars) and *Thysanoessa inermis* (Krøyer) in the southeastern Bering Sea,” Polar Res. **10**(2), 461-478.

Stanton, T.K. (1988a). “Sound scattering by cylinders of finite length I: Fluid cylinders.” J. Acoust. Soc. Am. **83**, 55-63.

Stanton, T.K. (1988b). “Sound scattering by cylinders of finite length II. Elastic cylinders.” J. Acoust. Soc. Am. **83**, 64-67.

Stanton, T.K. (1989). “Sound scattering by cylinders of finite length III: Deformed cylinders.” J. Acoust. Soc. Am. **86**, 691-705.

Stanton, T.K., Chu, D. Wiebe, P.H., Clay, C.S. (1993a). “Average echoes from randomly oriented random-length finite cylinders: Zooplankton models.” J. Acoust. Soc. Am. **96**(4), 3463-3472.

Stanton, T.K., Clay, C.S., and Chu, D. (1993b). “Ray representation of sound scattering by weakly scattering deformed fluid cylinders: Simple physics and application to zooplankton.” Journal of the Acoustical Society of America. **94**(6), 3454-3462.

Stanton, T.K., Weibe, P.H., Chu, D., Benfield, M.C., Scanlon, L., Martin, L.V. and Eastwood, R.L. (1994). “On acoustic estimates of biomass,” ICES J. Mar. Sci. **51**, 505-512.

Stanton, T.K., Chu, D., and Wiebe, P.H. (1996). “Acoustic scattering characteristics of several zooplankton groups,” ICES J. Mar. Sci. **53**, 289-295.

Stanton, T.K., Wiebe, P.H., Chu, D. (1998a). “Differences between sound scattering by weakly scattering spheres and finite-length cylinders with applications to sound scattering by zooplankton.” J. Acoust. Soc. Am. **103**(1), 254-264.

Stanton, T.K., Chu, D, Wiebe, P.H. (1998b). “Sound scattering by several zooplankton groups. II. Scattering models.” J. Acoust. Soc. Am. **103**(1), 236-253.

Stanton, T.K., and Chu, D. (2000). “Review and recommendations for the modeling of acoustic scattering by fluid-like elongated zooplankton: euphausiids and copepods,” ICES J. Mar. Sci. **57**, 793-807.

Taylor, J.R. (1982). “An introduction to error analysis: The study of uncertainties in physical measurements,” University Science Books, Mill Valley, CA. pp. 52-74.

Traynor, J.J. (1996). “Target-strength measurements of walleye pollock (*Theragra*

chalcogramma) and Pacific whiting (*Merluccius productus*)," ICES J. Mar. Sci. **53**(2), 253-258.

Urick, R.J. (1983). Principles of underwater sound, 3rd edition. McGraw-Hill, Inc. Peninsula Publishing, Los Altos, California.

Warren, J.D., Stanton, T.K, McGehee, D.E. and D. Chu. (2002). "Effect of animal orientation on acoustic estimates of zooplankton properties." IEEE J. of Ocean. Eng. **27**(1), 130-138.

Warren, J.D., and Wiebe, P.H. (2008). "Accounting for biological and physical sources of acoustic scattering improves estimates of zooplankton biomass." Can. J. of Fish. and Aqu. Sci. **65**, 1321-1333. doi:10.1139/F08-047

Warren, J.D., and Smith, J.N. (2007). "Density and sound speed of two gelatinous zooplankton: ctenophore (*Mnemiopsis leidyi*) and lion's mane jellyfish (*Cyanea capillata),*" J. Acoust. Soc. Am. **122**(2), 574-580.

Watkins, J.L. and A.S. Brierly. (1996). "A post-processing technique to remove background noise from echo integration data." ICES J. Mar. Sci. **53**, 339-344.

Wespestad, V.G., Fritz, L.W., Ingraham, W.J., Megrey, B.A. (2000). "On relationships between cannibalism, climate variability, physical transport, and recruitment success of Bering Sea walleye pollock (*Theragra chalcogramma*)." ICES J. of Mar. Sci. **57**, 272-278.

Wiebe, P.H., Morton, A.W., Bradley, A.M., Backus, R.H., Craddock, J.E., Barber, V., Cowles, T.J., and G.R. Flierl. (1985). "New developments in the MOCNESS, an apparatus for sampling zooplankton and micronekton." Marine Biology. **87**, 313-323.

Wiebe, P.H., Stanton, T.K., Benfield, M.C., Mountain, D.G., and Greene, C.H. (1997). "High-frequency acoustic volume backscattering in the Georges Bank Coastal Region and its interpretation using scattering models," IEEE J. Ocean. Eng. **22**(3), 445-464.

Wiebe, P.H., Chu, D., Kaartvedt, S., Hundt, A., Melle, W., Ona, E., and Batta-Lona, P. (2009). "The acoustic properties of *Salpa thompsoni*." ICES J. of Mar. Sci. 0; fsp263v2-fsp263.